Zoological Journal of the Linnean Society, 2024, **200**, 505–531
https://doi.org/10.1093/zoolinnean/zlad082
Advance access publication 16 August 2023
Original Article

OXFORD

Original Article

Hiding in the mists: molecular phylogenetic position and description of a new genus and species of snake (Dipsadidae: Xenodontinae) from the remote cloud forest of the Lost World

Philippe J. R. Kok[1,2,*] and D. Bruce Means[3,4]

[1]Department of Ecology and Vertebrate Zoology, Faculty of Biology and Environmental Protection, University of Łódź, 12/16 Banacha Street, Łódź 90-237, Poland
[2]Department of Life Sciences, The Natural History Museum, Cromwell Road, London SW7 5BD, United Kingdom
[3]Coastal Plains Institute and Land Conservancy, 46 Kinsey Road, Crawfordville, FL 32327, United States
[4]Department of Biological Science, Florida State University, 319 Stadium Drive, Tallahassee, FL 32304, United States

[*]Corresponding author. E-mail: philippe.kok@biol.uni.lodz.pl; philippe.kok@nhm.ac.uk; pjrkok@gmail.com

ABSTRACT

Pantepui *s.l.* is a remote, biodiverse region of ~400 000 km^2 containing at least five endemic reptile genera and a number of ancient vertebrate lineages. Here, we describe an additional endemic snake genus and species, ***Paikwaophis kruki* gen. nov., sp. nov.** (Dipsadidae: Xenodontinae), recently collected in the Pantepui cloud forest that sits at the base of the steep cliffs of Roraima-tepui and Wei-Assipu-tepui (table mountains of the Eastern Tepui Chain) in Guyana, South America. Multilocus molecular data strongly support ***Paikwaophis* gen. nov.** to be most closely related to *Xenopholis* Peters, 1869, although both genera are strikingly different morphologically. Osteological and other phenotypic data suggest that *Paikwaophis* is semi-fossorial; its diet includes minute lizards. *Paikwaophis* is currently the only known Pantepui endemic snake genus. The immature female holotype is the only known specimen.

Keywords: anatomy; *BDNF* nuDNA gene; *c-mos* nuDNA gene; *cytb* mtDNA gene; Guiana Shield; Guyana; 12S rRNA gene; 16S rRNA gene; *ND4* mtDNA gene; osteology

INTRODUCTION

With almost 1600 described snake species, the Neotropics are seemingly richer than any other tropical region (Raven *et al.* 2020). The family Dipsadidae (or as Dipsadinae, a subfamily of Colubridae, e.g. Pyron *et al.* 2011) currently contains > 800 extant species (Uetz 2022) and is the largest radiation of American snakes, with most genera occurring in the Neotropical region (Vidal *et al.* 2010, Grazziotin *et al.* 2012). Phylogenetic studies of the Dipsadidae have been based mostly on molecular and hemipenial characters to resolve supra- and intergeneric relationships (e.g. Vidal *et al.* 2010, Grazziotin *et al.* 2012, Zaher and Prudente 2020).

Located in the western Guiana Shield (Fig. 1), Pantepui (Mayr and Phelps 1967, McDiarmid and Donnelly 2005, Kok 2013) is a distinctive Neotropical palaeosurface (pre-Pleistocene landscape) that has been shaped by the physical erosion and deep chemical weathering of the extensive Roraima Supergroup (Priem *et al.* 1973, Briceño *et al.* 1990, Gibbs and Barron 1993, Santos *et al.* 2003). The term Pantepui was originally coined by Mayr and Phelps (1967) to characterize the high-elevation, meso- or microthermic life zones (> 1500 m a.s.l.) of the Guiana Shield highlands (Huber 1995). To reflect the biogeography and the biotic interactions in the area better, some authors extended this arbitrary definition to include the intervening lowlands and uplands, covering an area that probably corresponds roughly to a former ancient, large continuous plateau that was gradually eroded and dissected into many isolated table mountains locally called 'tepuis' (e.g. Steyermark 1979, 1982, Kok 2010, 2013). Pantepui is traditionally seen as one of the most

Received 11 January 2023; revised 2 June 2023; accepted 5 June 2023

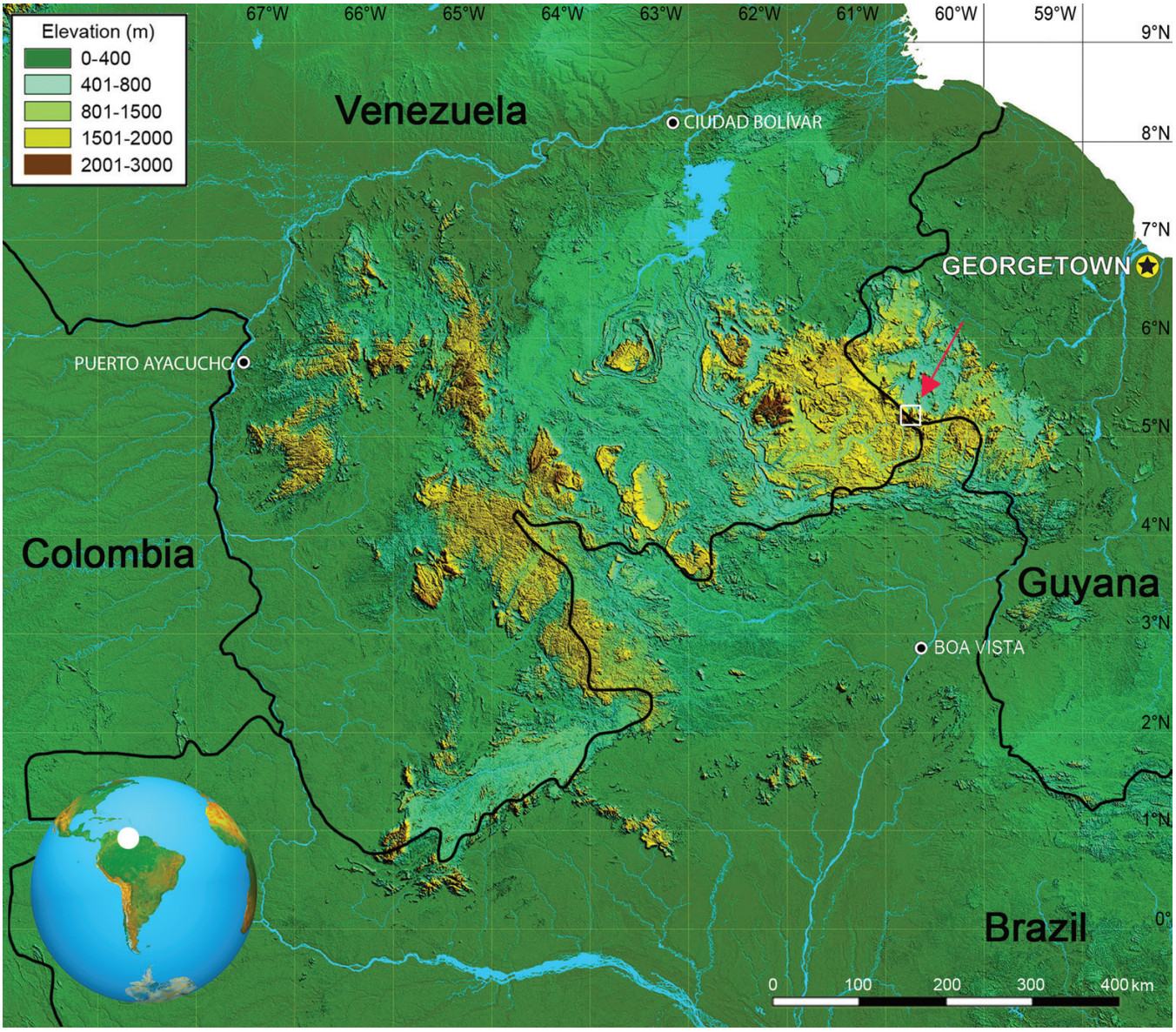

Figure 1. Map of the Pantepui biogeographical region and its location in South America (lower left inset). The red arrow points to a white rectangle depicting the area shown in Figure 2.

important centres of endemism in the Neotropics (Berry *et al.* 1995, Davis *et al.* 1997). However, although this mostly pristine region is renowned for high endemism and biodiversity (in particular, at genus and higher ranks of amphibians and reptiles), with the co-occurrence of several early branching lineages, it is often neglected as a cohesive ecoregion (e.g. Olson *et al.* 2001). A Pantepui origin, with subsequent dispersal to the lowlands, has been assumed or demonstrated in some amphibians, and the region seems to have acted as a source and sink for Neotropical biodiversity (e.g. Kok 2013, Kok *et al.* 2017, Vacher *et al.* 2017, Fouquet *et al.* 2021). Pantepui currently harbours one endemic amphibian family (Ceuthomantidae; Heinicke *et al.* 2009), one endemic lizard subfamily (Riolaminae; Kok 2015), eight endemic amphibian genera (*Ceuthomantis* Heinicke, Duellman, Trueb, Means, MacCulloch and Hedges, 2009, *Dischidodactylus* Lynch, 1979, *Metaphryniscus* Señaris, Ayarzagüena and Gorzula, 1994, *Minyobates* Myers, 1987, *Myersiohyla* Faivovich, Haddad, Garcia, Frost, Campbell and Wheeler, 2005, *Nesorohyla* Pinheiro, Kok, Noonan, Means, Haddad and Faivovich, 2018, *Oreophrynella* Boulenger, 1895 and *Stefania* Rivero, 1968; Boulenger 1895, Rivero 1968, Lynch 1979, Myers 1987, Señaris *et al.* 1994, Faivovich *et al.* 2005, Heinicke *et al.* 2009, Kok 2009a, 2013, Kok *et al.* 2016, 2017, Pinheiro *et al.* 2018) and five endemic reptile genera (*Adercosaurus* Myers and Donnelly, 2001; *Kaieteurosaurus* Kok, 2005; *Pantepuisaurus* Kok, 2009; *Riolama* Uzzell, 1973 and *Yanomamia* Pellegrino, Brunes, Souza, Laguna, Ávila-Pires, Hoogmoed and Rodrigues, 2018; Uzzell 1973, Myers and Donnelly 2001, Kok 2005, 2009b, 2015, Pellegrino *et al.* 2018). This does not include several still undescribed putative genera of frogs and lizards as reported by McDiarmid and Donnelly (2005), and P.J.R.K. is working on the description of two new endemic amphibian families (Fouquet *et al.*, in prep.), three new endemic

amphibian genera (Fouquet *et al.*, in prep.; Recoder *et al.*, in prep.) and one new endemic lizard genus (Kok *et al.*, in prep.) from the region.

A series of table mountains in Guyana trends from south-east to north-west along the border with Brazil and Venezuela. Rising to > 2800 m a.s.l., the queen of these mesas is Roraima-tepui [of Arthur Conan Doyle's (1912) Lost World fame], on whose summit the borders of all three countries meet. Because of their remoteness and summit-fringing cliffs, the summits have been explored mostly by helicopter expeditions, but the main species richness occurs in the dense cloud forests on tepui flanks, which can often be accessed only by foot. Since 2003, we have been conducting herpetological biodiversity research during five expeditions into the headwater tributaries of the Paikwa River drainage basin between Roraima-tepui and its eastern sister tepui, Wei-Assipu-tepui. On a 2021 herpetological/climbing expedition to the summit of Wei-Assipu in Guyana (Synnott 2022), 138 specimens of anurans, 13 lizards and nine snakes were collected on an elevational transect from Double Drop Falls to the base of the vertical cliffs of Wei-Assipu-tepui (Fig. 2). Among these specimens was a small dipsadid-like snake that could not be assigned to any known Colubroidea genus based on external morphology.

To assess the molecular phylogenetic position of this enigmatic snake, we estimated maximum likelihood (ML) and Bayesian phylogenies for a representative set of Dipsadidae using a multi-gene alignment including our specimen. We also μCT-scanned (μCT = micro-computed tomography) and analysed the osteology of the putative new taxon. Based on these data, we conclude that this peculiar snake should be described as a new genus and a new species of Dipsadidae (Xenodontinae), namely *Paikwaophis kruki*.

MATERIALS AND METHODS

Molecular data

Tissue sampling and DNA extraction, amplification and sequencing

Genomic DNA was isolated from a small tissue sample taken from the preserved specimen (whole animal fixed in 99% ethanol in the field). The tissue sample was immediately digested overnight at 56°C in a solution of 5 μL of proteinase K and 100 μL of lysis buffer (100 mM NaCl, 100 mM Tris, 25 mM EDTA and 0.5% SDS). DNA extraction was performed using Sera-Mag SpeedBeads (Thermo Fisher Scientific) at a concentration of ~1.7× (105 μL of digested tissue to 180 μL of beads) and eluted into 200 μL of 10 mM Tris buffer. Using polymerase chain reaction (PCR; for primers and PCR conditions, see Table 1), we amplified fragments of four genes of the mitochondrial DNA (mtDNA): the 16S ribosomal RNA gene (16S), the 12S ribosomal RNA gene (12S), the protein-coding genes cytochrome *b* (*cytb*) and NADH dehydrogenase subunit 4 (*ND4*); and two protein-coding genes of the nuclear DNA (nuDNA): brain-derived neurotrophic factor (*BDNF*) and oocyte maturation factor MOS (*c-mos*). The PCR amplifications were confirmed on a 1% agarose gel, and negative controls were run on all amplifications to exclude contamination. The PCR products were purified, then Sanger sequenced (along both strands using the same primers used for PCR) at the Natural History Museum's (NHM, London, UK) sequencing facility. Chromatograms were assembled and edited in CodonCode Aligner v.10.0.2 (Codon Code Corporation, Centerville, MA, USA).

Sequence alignment and phylogenetic analyses

Based on best gene coverage and the availability on GenBank, we selected one to three species per dipsadid genus and combined our specimen with 113 additional ingroup taxa (Table 2). The tree was rooted with *Coluber constrictor* Linnaeus, 1758 (Colubridae) as an outgroup. New sequences have been catalogued in GenBank (Table 2). Each gene was aligned independently using MAFFT v.7.490 (Katoh and Standley 2013) on the CIPRES Science Gateway (Miller *et al.* 2010), with appropriate strategies selected automatically. Ambiguously aligned regions in the 12S and 16S alignments were excluded manually, and the six genes were concatenated in Mesquite v.3.70 (Maddison and Maddison 2016), reaching a final dataset of 3772 nucleotide sites and 115 terminals representing 115 species and 93 genera. We divided our dataset into 14 partitions: one for the 12S, one for the 16S and one for each codon position of the protein-coding genes. The models of nucleotide evolution and best-fitting partition schemes were determined using PartitionFinder v.2.1.1 (Lanfear *et al.* 2017), under the Bayesian information criterion (BIC) and the greedy algorithm (Lanfear *et al.* 2017). The best scheme indicated five different best-fitting nucleotide substitution models (Table 3). Using this alignment, we conducted phylogenetic analyses simultaneously using ML and Bayesian inference (BI). The ML analysis was performed on the IQ-TREE Web Server using IQ-TREE v.1.6.12 (Trifinopoulos *et al.* 2016), with the substitution model set to 'auto' (Kalyaanamoorthy *et al.* 2017) and specifying FreeRate heterogeneity to generate a ML tree with 1000 ultrafast bootstrap replicates (Hoang *et al.* 2018). The BI analysis was performed with MrBayes v.3.2.7a (Ronquist *et al.* 2012) on CIPRES (Miller *et al.* 2010). Clade credibility was estimated using Bayesian posterior probabilities (PP) under the best partitioning schemes. Four parallel Markov chain Monte Carlo (MCMC) runs were performed, with a length of 2×10^7 generations, a sampling frequency of 1 per 1000 generations, and a burn-in of the first 5000 saved trees. Convergence of the parallel runs was confirmed by split frequency SDs (< 0.01) and potential scale reduction factors (~1.0) for all model parameters, as reported by MrBayes. Tracer v.1.7.2 (Rambaut *et al.* 2018) was used to confirm convergence of all analyses by plotting the log-likelihood values against the generation time for each run. Effective sample sizes (ESS) of all parameters were largely > 200, indicating stationarity and adequate sampling sizes. Consensus trees were visualized and edited with FigTree v.1.4.4 (Rambaut 2016).

Additional material examined

Xenopholis scalaris (Wucherer, 1861): South America, Bolivia, BMNH 1901.8.2.34, BMNH 1895.11.21.41; Brazil, BMNH 1946.1.8.66; Ecuador, BMNH 1880.12.8.133; French Guiana, Camp Patawa, NHMUK 2023.3195 (BMNH and NHMUK = Natural History Museum, London, UK).

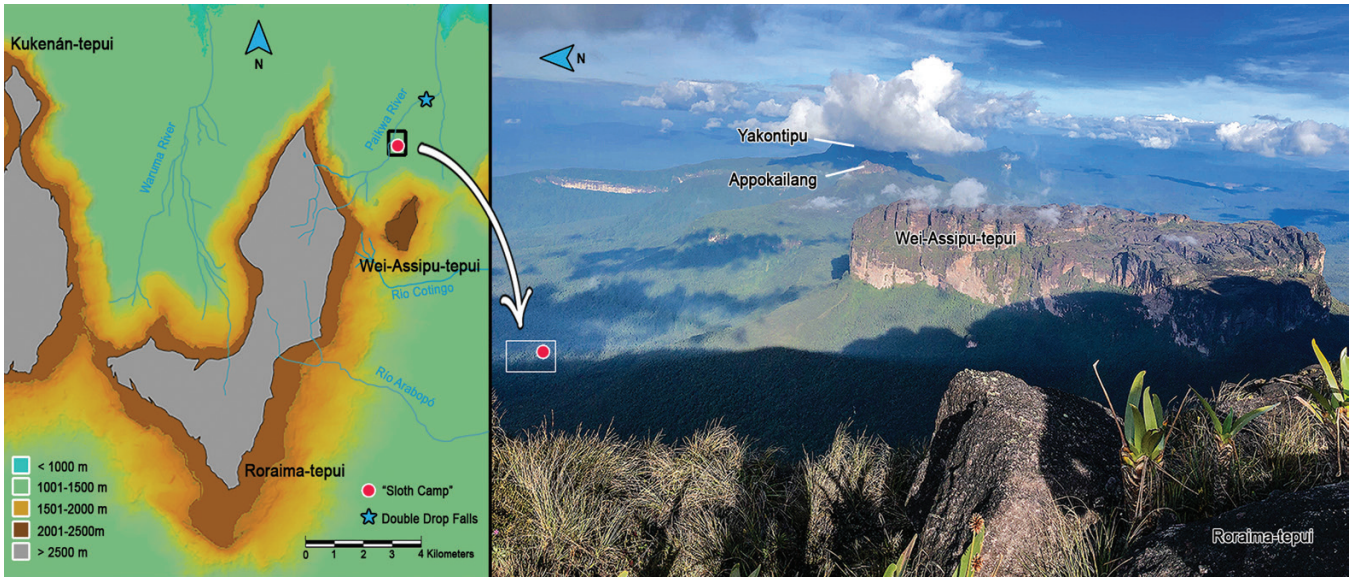

Figure 2. Left, terra typica of ***Paikwaophis kruki***. Right, the Eastern Tepui Chain in Guyana as seen from the summit of Roraima-tepui, facing east (10 March 2019), with the type locality of ***Paikwaophis kruki*** depicted as a red dot. Photograph by P.J.R.K.

Morphological data

Morphometrics and sex determination

Morphological examinations of our specimen were performed under a Leica M205C stereomicroscope by P.J.R.K. The specimen was fixed in the field in 99% ethanol and later transferred to 70% ethanol for permanent preservation. The specimen has been deposited at the Royal Belgian Institute of Natural Sciences (RBINS), Brussels, Belgium (*RBINS 2734*; see 'Holotype' below).

Terminology for cephalic scales and scale counts followed Dowling (1951) and Peters (1964). Measurements were taken to the nearest 0.01 mm (rounded to 0.1 mm) with digital callipers (MarCal 16 EWRi), except for the snout–vent length (SVL; from tip of snout to posterior margin of cloacal plate) and tail length (TaL; from posterior margin of cloacal plate to tip of tail), which were measured with a ruler to the nearest 0.1 mm. Other measurements were abbreviated as follows: TL, total length = SVL + TaL; HL, head length (from tip of snout to posterior margin of the mandible); HW, maximum head width; ED, maximum eye horizontal length; DSN, distance from tip of snout to nostril; DNE, distance from nostril to anterior margin of eye; SnL, snout length (from tip of snout to anterior margin of eye); RW, maximum rostral width; and RH, maximum rostral height. Selected meristic characters were abbreviated as follows: DSR, dorsal scale rows (counted around the body at a head's length behind the head, at midbody and at a head's length before the cloaca); SL, supralabials; IL, infralabials; PrO, preoculars; PtO, postoculars; SuO, supraoculars; IN, internasals; LoR, loreal; TMP, temporals; CS, chinshields; V, ventral scales; and SC, subcaudals.

The sex of the holotype was determined by dissection and examination of the gonads and by absence of hemipenes.

Micro-computed tomography scanning and three-dimensional reconstructions

Given the results of the molecular phylogenetic analyses (see 'Phylogenetic relationships' below), we focused our osteological investigations on our specimen and two specimens of *Xenopholis scalaris*: a syntype, BMNH 1946.1.8.66 (see Discussion); and a specimen recently collected in French Guiana, NHMUK 2023.3195. Snakes underwent µCT scanning at the NHM's CT laboratory facility using either a Zeiss Versa 520 (for the head of our specimen) or a Nikon HMX225 (for all other µCT scans). Osteological images were exported from the virtual three-dimensional models, which were reconstructed and segmented by P.J.R.K. using VGStudio MAX v.2.1. All µCT scans have been deposited on the MorphoSource platform. Osteological terminology followed Cundall and Irish (2008).

Morphological comparisons

Morphological comparisons were based on examination of museum specimens (see above, 'Additional material examined') and a comprehensive review of published descriptions and systematic revisions of dipsadid genera and species (> 100 references).

Eight known genera of Xenodontinae were not included in our phylogenetic analyses owing to the lack of DNA sequences in GenBank and the lack of material for DNA extraction. These genera are as follows: *Amnesteophis* Myers, 2011, *Baliodryas* Zaher and Prudente, 2020, *Cenaspis* Campbell, Smith and Hall, 2018, *Cercophis* Fitzinger, 1843, *Coronelaps* Lema and Hofstadler-Deiques, 2010, *Ditaxodon* Hoge, 1958, *Incaspis* Donoso-Barros, 1974, *Lioheterophis* Amaral, 1935 and *Saphenophis* Myers, 1973. The molecular phylogenetic relationships of these genera (except *Incaspis*; see Arredondo *et al.* 2020) are thus unknown, and we carefully compared the morphology of our specimen with the original descriptions of these taxa to exclude potential morphological affinities that could contradict the hypothesis that our specimen should be described in a new genus (see the comparisons subsections below).

Table 1. Primers and PCR conditions.

Locus	Gene type	Primer name	Sequence (5′–3′)	Annealing temperature (°C)	Primer source
16S[a]	Mitochondrial	Forward: L2510	CCGACTGTTTAMCAAAAACA	54	Palumbi *et al.* (1991)
		Reverse: H3056	CTCCGGTCTGAACTCAGATCACGTAGG	54	Hedges (1994)
12S[a]	Mitochondrial	Forward: L1091mod	CAAACTAGGATTAGATACCCTACTAT	51	Kocher *et al.* (1989)
		Reverse: H1157mod	GTACRCTTACCWTGTTACGACTT	51	Knight and Mindell (1994)
cytb[b]	Mitochondrial	Forward: 703Botp.mod	TCAAAYATCTCAACCTGATGAAAYTTYGG	54	Pook *et al.* (2000)
		Reverse: MVZ16p.mod	GGCAAATAGGAAGTATCAYTCTGGYTT	54	Pook *et al.* (2000)
ND4[b]	Mitochondrial	Forward: ND4	TGACTACCAAAAGCTCATGTAGAAGC	50	Forstner *et al.* (1995)
		Reverse: LEU	TACTTTTACTTGGATTTGCACCA	50	Forstner *et al.* (1995)
BDNF[b]	Nuclear	Forward: BDNFF	GACCATCCTTTTCCTKACTATGGTTATTTCATACTT	54	Leaché and McGuire (2006)
		Reverse: BDNFR	CTATCTTCCCCTTTAATGGTCAGTGTACAAAC	54	Leaché and McGuire (2006)
c-mos[b]	Nuclear	Forward: S77	CATGGACTGGGATCAGTTATG	50	Lawson *et al.* (2005)
		Reverse: S78	CCTTGGGTGTGATTTTCTCACCT	50	Lawson *et al.* (2005)

[a]96°C for 3 min; 40 × 95°C for 30 s, annealing for 60 s, 72°C for 1 min; 1 × 72°C for 10 min.
[b]94°C for 4 min; 40 × 94°C for 60 s, annealing for 60 s, 72°C for 1 min; 1 × 72°C for 10 min.

RESULTS

Phylogenetic relationships

The ML and BI analyses of the multi-gene matrix resulted in similar tree topologies with no major conflict (i.e. no highly supported alternatives) and were mostly congruent with existing phylogenetic studies of Dipsadidae (e.g. Grazziotin *et al.* 2012, Zaher *et al.* 2019, Moraes *et al.* 2021). For brevity and clarity, we illustrate only the BI tree topology (Fig. 3; unedited phylogenetic trees are provided as Supporting Information, Figs S1, S2).

The phylogenetic analyses recovered our specimen as sister to *Xenopholis* (Xenodontinae) with strong support (ML = 100; BI = 100). Our specimen + *Xenopholis* were recovered as sister to the tribe Pseudoboini with moderate support in the ML analysis (ML = 88) and low support in the BI analysis (BI = 43).

Morphological characters

A combination of morphological characters unambiguously distinguishes the new genus from all other known Xenodontinae genera (see 'Generic diagnosis' below). Notably, we found striking differences in both the external morphology and the osteological characters between our specimen and the three known species of *Xenopholis* (sister genus) and from the eight known genera of Xenodontinae that were not included in our phylogenetic analyses, warranting the erection of a new monotypic genus (see the comparisons subsections below).

SYSTEMATICS

Family Dipsadidae Bonaparte, 1838

Subfamily Xenodontinae Cope, 1893

Paikwaophis gen. nov.

(Figs 4–13)

Zoobank registration: urn:lsid:zoobank.org:act:FF55996A-80A3-4189-838F-269A47BBD9F0.

Type species: Paikwaophis kruki sp. nov.

Etymology: The generic name is derived from the river name 'Paikwa' (referring to the type locality) and the Greek '*ophis*' (meaning snake).

Generic diagnosis: Paikwaophis can be differentiated from all other Xenodontinae (and Dipsadidae) by the combination of the following morphological characters: head poorly distinct from neck; body robust, slightly wider than high; tail short, ~13% of total length in female; snout short and blunt; rostral wider than high, visible from above; undivided nasal; paired internasals; paired prefrontals; subtriangular frontal; absence of loreal; presence of minute cephalic sensory pits; eye medium in size, with vertically oval pupil, iris dark reddish orange; single supraocular; one preocular, two postoculars; three rows of temporals; chinshields medium in size, anterior chinshields projecting frontolaterally; body scales rhomboid, smooth, lacking keels or apical pits, 17 dorsal scale rows without reduction; subcaudals paired; anal

Table 2. List of taxa used in the molecular phylogenetic analyses, with GenBank accession numbers. Sequences newly generated are in bold.

Family	Subfamily	Tribe	Genus	Species	16S	12S	*cytb*	*ND4*	*BDNF*	*c-mos*
Colubridae			*Coluber*	*constrictor*	L01770	L01765	EU180432	AY487040	JQ599015	AY486937
Dipsadidae	Carpophiinae		*Carphophis*	*amoenus*	AY577022	AY577013	AF471067			DQ112082
Dipsadidae	Carpophiinae		*Contia*	*tenuis*	AY577030	AY577021	GU112401	AF402658	GU112363	AF471134
Dipsadidae	Carpophiinae		*Diadophis*	*punctatus*	KX694636	AY577015	EU193670	EU194025	EU402637	AF471122
Dipsadidae	Dipsadinae		*Chapinophis*	*xanthocheilus*			JX398603	JX398450		
Dipsadidae	Dipsadinae		*Adelphicos*	*quadrivirgatus*			GQ895853			GQ895796
Dipsadidae	Dipsadinae		*Amastridium*	*sapperi*			GQ334479	GQ334580		
Dipsadidae	Dipsadinae		*Amastridium*	*veliferum*	MH140469					GQ895797
Dipsadidae	Dipsadinae		*Atractus*	*albuquerquei*	GQ457726	GQ457783	JQ598918		JQ599009	GQ457845
Dipsadidae	Dipsadinae		*Chersodromus*	*liebmanni*			JX398604	JX398451		
Dipsadidae	Dipsadinae		*Coniophanes*	*fissidens*	MH140663		EF078538	JX398452		
Dipsadidae	Dipsadinae		*Cryophis*	*hallbergi*			GQ895863	EF078544		GQ895807
Dipsadidae	Dipsadinae		*Dipsas*	*catesbyi*	Z46496	JQ598805	JQ598926	EF078585	JQ599021	JQ598977
Dipsadidae	Dipsadinae		*Enuliophis*	*sclateri*	MH140724		JX398635	JX398485		
Dipsadidae	Dipsadinae		*Enulius*	*flavitorques*	MH140725		JX398636	JX398486		
Dipsadidae	Dipsadinae		*Geophis*	*godmani*	JQ598877	JQ598814	JQ598932		JQ599026	
Dipsadidae	Dipsadinae		*Hydromorphus*	*concolor*			GQ895874	JX398490		GQ895817
Dipsadidae	Dipsadinae		*Hypsiglena*	*torquata*	EU728591	EU728591	EU728591	EU728591		AF471159
Dipsadidae	Dipsadinae		*Hypsiglena (Eridiphas)*	*slevini*	EU728584	EU728584	EU728584	EU728584		
Dipsadidae	Dipsadinae		*Imantodes*	*cenchoa*	EU728586	EU728586	EU728586	EU728586	EU402643	GQ457865
Dipsadidae	Dipsadinae		*Leptodeira*	*annulata*	GQ457746	GQ457806	FJ416713	FJ416787	FJ433998	AF544690
Dipsadidae	Dipsadinae		*Ninia*	*atrata*	JQ598882	GQ457814	JQ598937	GQ334659	JQ599037	GQ457874
Dipsadidae	Dipsadinae		*Pliocercus*	*euryzonus*	KX660165		KX660440	KX660568		KX660304
Dipsadidae	Dipsadinae		*Pseudoleptodeira*	*latifasciata*	EU728579	EU728579	EU728579	EU728579		
Dipsadidae	Dipsadinae		*Rhadinaea*	*decorata*	MH140927					
Dipsadidae	Dipsadinae		*Sibon*	*nebulatus*	EU728583	EU728583	EU728583	EU728583		AF544736
Dipsadidae	Dipsadinae		*Tretanorhinus*	*variabilis*	AF158529	AF158460	JX398722	JX398592		
Dipsadidae	Dipsadinae		*Trimetopon*	*gracile*	GU018178	GU018160	JX398723	JX398593		
Dipsadidae	Dipsadinae		*Tropidodipsas*	*sartorii*			JX398718	JX398587		
Dipsadidae	Dipsadinae		*Urotheca*	*guentheri*			JX398726	JX398596		
Dipsadidae	*incertae sedis*		*Farancia*	*abacura*	Z46491	Z46467	U69832	DQ902307		AF471141
Dipsadidae	*incertae sedis*		*Heterodon*	*platirhinos*	AY577028	AY577019	GU112412	AF402659	EU402641	JQ598986
Dipsadidae	*incertae sedis*		*Thermophis*	*zhaoermii*	GQ166168	GQ166168	GQ166168	GQ166168		KP777529
Dipsadidae	Xenodontinae		*Paikwaophis*	*kruki*	**OR075194**	**OR075146**	**OR069382**	**OR069383**	**OR069380**	**OR069381**
Dipsadidae	Xenodontinae	Alsophiini	*Alsophis*	*antillensis*	FJ416702	FJ416691	FJ416726	FJ416800	JQ599005	
Dipsadidae	Xenodontinae	Alsophiini	*Alsophis*	*rijgersmaei*	FJ416708	FJ416697	FJ416729	FJ416803		

Table 2. Continued

Family	Subfamily	Tribe	Genus	Species	16S	12S	*cytb*	*ND4*	*BDNF*	*c-mos*
Dipsadidae	Xenodontinae	Alsophiini	*Arrhyton*	*dolichura*	AF158507	AF158438	FJ416721	FJ416795		
Dipsadidae	Xenodontinae	Alsophiini	*Arrhyton*	*procerum*	AF158521	AF158452	FJ416723	FJ416797		
Dipsadidae	Xenodontinae	Alsophiini	*Borikenophis*	*portoricensis*	AF158517	FJ416696	AF471085	U49308	JQ599012	AF471126
Dipsadidae	Xenodontinae	Alsophiini	*Borikenophis*	*variegatus*	FJ416711	FJ416700	FJ416734	FJ416808		
Dipsadidae	Xenodontinae	Alsophiini	*Caraiba*	*andreae*	AF158511	AF158442	FJ416743	FJ416817		
Dipsadidae	Xenodontinae	Alsophiini	*Cubophis*	*cantherigerus*	AF158475	AF158405	AF544669	FJ416818	FJ433999	AF544694
Dipsadidae	Xenodontinae	Alsophiini	*Cubophis*	*caymanus*	FJ416704	FJ416693	FJ416745	FJ416820		
Dipsadidae	Xenodontinae	Alsophiini	*Haitiophis*	*anomalus*	FJ666092	FJ666091				
Dipsadidae	Xenodontinae	Alsophiini	*Hypsirhynchus*	*ferox*	AF158515	AF158447	GQ895875	FJ416816		GQ895818
Dipsadidae	Xenodontinae	Alsophiini	*Hypsirhynchus*	*parvifrons*	AF158510	AF158441	FJ416740	FJ416814		
Dipsadidae	Xenodontinae	Alsophiini	*Ialtris*	*dorsalis*	AF158525	AF158456	FJ416735	FJ416809		
Dipsadidae	Xenodontinae	Alsophiini	*Magliophis*	*exiguum*	AF158526	FJ416694	AF471071	FJ416798		AF471117
Dipsadidae	Xenodontinae	Alsophiini	*Uromacer*	*catesbyi*	AF158523	AF158454	FJ416714	FJ416788		
Dipsadidae	Xenodontinae	Caaeteboiini	*Caaeteboia*	*amarali*	GQ457747	GQ457807	JQ598921			GQ457867
Dipsadidae	Xenodontinae	Conophiini	*Conophis*	*lineatus*	JQ598865	GQ457788	JQ598924		JQ599016	JQ598975
Dipsadidae	Xenodontinae	Conophiini	*Manolepis*	*putnami*	JQ598881	JQ598820	JQ598936		JQ599035	JQ598988
Dipsadidae	Xenodontinae	Diaphorolepidini	*Diaphorolepis*	*wagneri*	KR814752		KT345360	KR814775		KR814764
Dipsadidae	Xenodontinae	Diaphorolepidini	*Synophis*	*bicolor*	KR814758	KR814751	KR814773			KR814769
Dipsadidae	Xenodontinae	Diaphorolepidini	*Synophis*	*calamitus*	KR814640	KR814622	KR814697	KR814711		KR814663
Dipsadidae	Xenodontinae	Echinantherini	*Echinanthera*	*melanostigma*	GU018174	JQ598806	JQ598928			
Dipsadidae	Xenodontinae	Echinantherini	*Echinanthera*	*undulata*	JQ598870	JQ598807	JQ598929		JQ599022	JQ598978
Dipsadidae	Xenodontinae	Echinantherini	*Sordellina*	*punctata*	JQ598903	JQ598843	JQ598956		JQ599052	JQ599000
Dipsadidae	Xenodontinae	Echinantherini	*Taeniophallus*	*affinis*	JQ598905	JQ598844	JQ598957		JQ599055	GQ457853
Dipsadidae	Xenodontinae	Echinantherini	*Taeniophallus*	*brevirostris*	GQ457734	GQ457793	JQ598958		JQ599056	GQ457854
Dipsadidae	Xenodontinae	Echinantherini	*Taeniophallus*	*nicagus*	KX694677	KX694562	KX694886		KX694766	KX694823
Dipsadidae	Xenodontinae	Elapomorphini	*Apostolepis*	*assimilis*	GQ457724	GQ457781			JQ599007	GQ457843
Dipsadidae	Xenodontinae	Elapomorphini	*Apostolepis*	*dimidiata*	GQ457725	GQ457782	JQ598917		JQ599008	GQ457844
Dipsadidae	Xenodontinae	Elapomorphini	*Elapomorphus*	*quinquelineatus*	GQ457735	GQ457794	JQ598930		JQ599023	GQ457855
Dipsadidae	Xenodontinae	Elapomorphini	*Phalotris*	*lemniscatus*	GQ457756	GQ457817	JQ598941		JQ599039	GQ457877
Dipsadidae	Xenodontinae	Elapomorphini	*Phalotris*	*nasutus*	GQ457757	GQ457818	GQ895880			GQ895822
Dipsadidae	Xenodontinae	Eutrachelophiini	*Arcanumophis*	*problematicus*	MH532901	MH513952	MH536833		MH536834	
Dipsadidae	Xenodontinae	Eutrachelophiini	*Eutrachelophis*	*papilio*	OK299146			OK334957		
Dipsadidae	Xenodontinae	Hydrodynastini	*Hydrodynastes*	*bicinctus*	GQ457742	GQ457802	JQ598935		JQ599030	GQ457862
Dipsadidae	Xenodontinae	Hydrodynastini	*Hydrodynastes*	*gigas*	GQ457743	GQ457803	GQ895873		JQ599031	GQ895816
Dipsadidae	Xenodontinae	Hydropsini	*Helicops*	*angulatus*	GQ457738	GQ457797	AF471037		MN032459	AF471160
Dipsadidae	Xenodontinae	Hydropsini	*Helicops*	*infrataeniatus*	GQ457740	GQ457799	JQ598933			GQ457859

Table 2. Continued

Family	Subfamily	Tribe	Genus	Species	16S	12S	*cytb*	*ND4*	*BDNF*	*c-mos*
Dipsadidae	Xenodontinae	Hydropsini	*Hydrops*	*triangularis*	GQ457744	GQ457804	AF471039		JQ599032	AF471158
Dipsadidae	Xenodontinae	Hydropsini	*Pseudoeryx*	*plicatilis*	GQ457765	GQ457826	GQ895885			GQ895826
Dipsadidae	Xenodontinae	*incertae sedis*	*Crisantophis*	*nevermanni*	GU018169	GU018152				
Dipsadidae	Xenodontinae	*incertae sedis*	*Xenopholis*	*scalaris*	JQ598915	JQ598854	GQ895897			JQ599002
Dipsadidae	Xenodontinae	*incertae sedis*	*Xenopholis*	*undulatus*	JQ598916	JQ598855				JQ599003
Dipsadidae	Xenodontinae		*Nothopsis*	*rugosus*	KR814760	GU018159	KR814770	KR814779		KR814768
Dipsadidae	Xenodontinae		*Rhadinella*	*godmani*			MZ520229	MZ520309	JQ599026	MZ520195
Dipsadidae	Xenodontinae		*Rhadinophanes*	*monticola*			JX398650	JX398498		
Dipsadidae	Xenodontinae		*Stichophanes*	*ningshaanensis*	KJ719252	KJ719252	KJ719252	KJ719252		KJ638718
Dipsadidae	Xenodontinae		*Tantalophis*	*discolor*			EF078541	EF078589		
Dipsadidae	Xenodontinae	Phylodryadini	*Chlorosoma*	*viridissimum*	AF158474	AF158419	AF236807			
Dipsadidae	Xenodontinae	Phylodryadini	*Philodryas*	*olfersii*	AF158484	JQ598830	JQ598945		JQ599041	JQ598993
Dipsadidae	Xenodontinae	Phylodryadini	*Xenoxybelis*	*argenteus*	GQ457780	GQ457842	JQ598944		JQ599040	GQ457899
Dipsadidae	Xenodontinae	Pseudoboini	*Boiruna*	*maculata*	JQ598862	GQ457785	GQ895855		JQ599011	GQ895799
Dipsadidae	Xenodontinae	Pseudoboini	*Clelia*	*clelia*	AF158472	AF158403				JQ598973
Dipsadidae	Xenodontinae	Pseudoboini	*Drepanoides*	*anomalus*	GQ457732	GQ457791	GQ895866			GQ895810
Dipsadidae	Xenodontinae	Pseudoboini	*Mussurana*	*bicolor*	GQ457729	GQ457787				GQ457849
Dipsadidae	Xenodontinae	Pseudoboini	*Oxyrhopus*	*guibei*	JQ627291	JQ598822	JQ598938		JQ599038	JQ598989
Dipsadidae	Xenodontinae	Pseudoboini	*Paraphimophis*	*rusticus*	JQ598864	JQ598802	JQ598923			JQ598974
Dipsadidae	Xenodontinae	Pseudoboini	*Phimophis*	*guerini*	GQ457761	GQ457822				GQ457882
Dipsadidae	Xenodontinae	Pseudoboini	*Pseudoboa*	*nigra*	GQ457764	AF544775	JQ598948		JQ599043	AF544729
Dipsadidae	Xenodontinae	Pseudoboini	*Rhachidelus*	*brazili*	JQ598897	JQ598837	JQ598952		JQ599048	
Dipsadidae	Xenodontinae	Pseudoboini	*Rodriguesophis*	*iglesiasi*	JQ598891	JQ598831	GQ895881			GQ895823
Dipsadidae	Xenodontinae	Pseudoboini	*Siphlophis*	*cervinus*	JQ598901	JQ598841	GQ895888			JQ598998
Dipsadidae	Xenodontinae	Pseudoboini	*Siphlophis*	*pulcher*	GQ457773	GQ457834	JQ598955		JQ599051	GQ457894
Dipsadidae	Xenodontinae	Psomophiini	*Psomophis*	*joberti*	GQ457768	GQ457829	GQ895887		JQ599046	GQ895828
Dipsadidae	Xenodontinae	Saphenophiini	*Pseudalsophis*	*elegans*	AF158470	AF158401	JQ598947		JQ599042	JQ598995
Dipsadidae	Xenodontinae	Tachymenini	*Calamodontophis*	*paucidens*	GQ457728	GQ457786				GQ457848
Dipsadidae	Xenodontinae	Tachymenini	*Gomesophis*	*brasiliensis*	GQ457737	GQ457796				
Dipsadidae	Xenodontinae	Tachymenini	*Pseudotomodon*	*trigonatus*	GQ457766	GQ457827				GQ457887
Dipsadidae	Xenodontinae	Tachymenini	*Ptychophis*	*flavovirgatus*	GQ457769	GQ457830				GQ457890
Dipsadidae	Xenodontinae	Tachymenini	*Tachymenis*	*peruviana*	GQ457774	GQ457835			JQ599054	GQ457895
Dipsadidae	Xenodontinae	Tachymenini	*Thamnodynastes*	*rutilus*	GQ457776	GQ457837				GQ457896
Dipsadidae	Xenodontinae	Tachymenini	*Thamnodynastes*	*strigatus*	JQ598907	JQ598847	JQ598959		JQ599057	KX660420
Dipsadidae	Xenodontinae	Tachymenini	*Tomodon*	*dorsatus*	GQ457777	GQ457838	GQ895892		JQ599059	GQ895833
Dipsadidae	Xenodontinae	Tropidodryadini	*Tropidodryas*	*serra*	JQ598908	JQ598848	JQ598961			

Table 2. Continued

Family	Subfamily	Tribe	Genus	Species	16S	12S	*cytb*	*ND4*	*BDNF*	*c-mos*
Dipsadidae	Xenodontinae	Tropidodryadini	*Tropidodryas*	*striaticeps*	GQ457778	GQ457839	AF236811		JQ599060	
Dipsadidae	Xenodontinae	Xenodontini	*Erythrolamprus*	*aesculapii*	GQ457736	GQ457795	GQ895871	MN703551	JQ599024	GQ895814
Dipsadidae	Xenodontinae	Xenodontini	*Erythrolamprus*	*miliaris*	AF158480	JQ598811	JQ598931		KX694720	JQ598982
Dipsadidae	Xenodontinae	Xenodontini	*Lygophis*	*elegantissiumus*	GQ457748	GQ457808				GQ457868
Dipsadidae	Xenodontinae	Xenodontini	*Lygophis*	*meridionalis*	GQ457750	GQ457810				GQ457870
Dipsadidae	Xenodontinae	Xenodontini	*Xenodon*	*histricus*	GQ457753	GQ457813	JQ598962		JQ599061	
Dipsadidae	Xenodontinae	Xenodontini	*Xenodon*	*merremi*	JQ598911	GQ457840	JQ598963		JQ599062	

entire; aglyphous, presence of a diastema; low number of teeth: 7 prediastemal maxillary teeth, 2 enlarged postdiastemal maxillary teeth, 8 pterygoid teeth, 5 palatine teeth, 12 dentary teeth; neural spines smooth, ungrooved and not laterally expanded; 175 trunk vertebrae; absence of hypapophyses on posterior vertebrae; caudal vertebrae with distinct haemapophyses; lacrimal foramen large and vertically ovoid; and postorbital bone highly reduced, free from the frontal bone.

Comparisons with known genera of Xenodontinae not included in our phylogenetic analyses: Paikwaophis is distinguished from *Amnesteophis* (assigned to the monotypic tribe Amnestophiini; Myers 2011) by, inter alia, the dentition: syncranterian (absence of a diastema), 25 maxillary teeth and 30 pterygoid teeth in *Amnesteophis* vs. diacranterian (presence of a diastema), 9 maxillary teeth and 8 pterygoid teeth in *Paikwaophis*.

Paikwaophis is distinguished from *Baliodryas* (assigned to the tribe Eutrachelophiini; Myers and McDowell 2014, Moraes *et al.* 2021) by, inter alia, the dentition: 25–28 maxillary teeth and 35–36 pterygoid teeth in *Baliodryas* vs. 9 maxillary teeth and 8 pterygoid teeth in *Paikwaophis*.

Paikwaophis is distinguished from the genus *Cenaspis* [unassigned to any tribe, seemingly endemic to the isolated highlands of western Chiapas in Mexico; the only known specimen has been found in the stomach of a *Micrurus nigrocinctus* (Girard, 1854); Campbell *et al.* 2018] by, inter alia, the state of the subcaudals and the maxillary dentition: single subcaudals in *Cenaspis* vs. divided subcaudals in *Paikwaophis*, and 10–15 maxillary teeth in *Cenaspis* vs. 9 maxillary teeth in *Paikwaophis*.

Paikwaophis is distinguished from *Cercophis* (unassigned to any tribe) by, inter alia, a short tail (13% of total length) vs. a long tail (42–54% of total length; Cunha and Nascimento 1982, Hoogmoed 2019) in *Cercophis*, and the maxillary dentition: 22 maxillary teeth in *Cercophis* vs. 9 maxillary teeth in *Paikwaophis*.

Paikwaophis is distinguished from *Coronelaps* (assigned to the tribe Elapomorphini; Lema and Hofstadler Deiques 2010) and *Ditaxodon* (assigned to the tribe Phylodryadini; Arredondo *et al.* 2020) by, inter alia, the dentition: opisthoglyphous (grooved fangs) in *Coronelaps* and *Ditaxodon* vs. aglyphous opisthodont (ungrooved fangs) in *Paikwaophis*.

Paikwaophis is distinguished from *Incaspis* (assigned to the tribe Incaspidini; Arredondo *et al.* 2020) by, inter alia, the dentition: 10–15 maxillary teeth in *Incaspis* vs. 9 maxillary teeth in *Paikwaophis* and the absence of apical pits in *Paikwaophis* (vs. one or two consistently present in *Incaspis*).

Paikwaophis is distinguished from *Lioheterophis* (unassigned to any tribe, monotypic, known only from the holotype collected in Campina Grande in north-eastern Brazil; Amaral 1935, Wallach *et al.* 2014) by, inter alia, the maxillary dentition: 17 maxillary teeth in *Lioheterophis* vs. 9 maxillary teeth in *Paikwaophis*; and a distinct difference in the number of dorsal scale rows: 21 with reduction in *Lioheterophis* vs. 17 without reduction in *Paikwaophis*.

Paikwaophis is distinguished from *Saphenophis* (assigned to the tribe Saphenophiini; Zaher *et al.* 1999) by, inter alia, the dentition: 19–22 maxillary teeth and 24–26 pterygoid teeth in *Saphenophis* (Myers 1973) vs. 9 maxillary teeth and 8 pterygoid teeth in *Paikwaophis*.

Table 3. Best partitioning scheme used for the Bayesian inference of phylogenetic relationships.

Subset	Best model	Partition names: gene(codon)
1	GTR+I+G	*cytb*(1), 12S, *ND4*(2)
2	GTR+I+G	16S
3	GTR+I+G	*ND4*(3), *cytb*(2)
4	GTR+G	*ND4*(1), *cytb*(3)
5	K80+I	*BDNF*(1), *BDNF*(2)
6	K80+I+G	*BDNF*(3)
7	K80+I+G	*c-mos*(2), *c-mos*(1)
8	HKY+G	*c-mos*(3)

Comparisons with the sister genus (Xenopholis): Although recovered as sister taxa with high support, *Paikwaophis* and *Xenopholis* (Figs 12–15) are strikingly different both morphologically and osteologically. Both genera are easily distinguished by, inter alia (non-exhaustive):

(i) The shape of the head and neck: marked neck and proportionally flatter/longer head in *Xenopholis* vs. neck poorly marked and short head in *Paikwaophis* (Figs 3, 4).
(ii) The presence of numerous minute cephalic sensory pits in *Paikwaophis* (absent in the *Xenopholis* specimens examined and not reported by Gomes *et al.* 2020).
(iii) The number of trunk vertebrae: 128–129 in *Xenopholis* vs. 175 in *Paikwaophis*.
(iv) The shape of the vertebrae: neural spines are expanded laterally, forming rugose shields divided by a median groove in *Xenopholis* (Hoge and Federsoni 1974) vs. smooth, ungrooved and not laterally expanded in *Paikwaophis* (Fig. 12); and hypapophyses on posterior vertebrae are absent in *Paikwaophis* (present in *Xenopholis*; Hoge and Federsoni 1974).
(v) The shape of the caudal vertebrae: caudal vertebrae have distinct haemapophyses in *Paikwaophis* (absent in *Xenopholis*).
(vi) The dentition: opisthoglyphous (grooved fangs) in *Xenopholis* (Gomes *et al.* 2020) vs. aglyphous opisthodont (ungrooved fangs) in *Paikwaophis* (Fig. 12), and a much higher number of teeth in *Xenopholis* (13–15 prediastemal maxillary teeth, 14–28 pterygoid teeth, 7–10 palatine teeth and 23–24 dentary teeth; Gomes *et al.* 2020) than in *Paikwaophis* (7 prediastemal maxillary teeth, 8 pterygoid teeth, 5 palatine teeth and 12 dentary teeth; Figs 7, 9, 10, 11, 15).
(vii) The shape and size of the lacrimal foramen: small and horizontally ovoid in *Xenopholis* vs. large and vertically ovoid in *Paikwaophis* (Fig. 13).
(viii) The shape and size of the postorbital bone: large and projecting ventrolaterally in *Xenopholis* vs. highly reduced, crescent-shaped in *Paikwaophis* (Figs 7, 15).

Comparisons with (near-) sympatric dipsadid genera with superficially similar morphology: In the Pantepui region (and northern Brazil) and based on superficial morphology/body plan and fossorial/semi-fossorial habits, *Paikwaophis* could be confused only with *Atractus* Wagler, 1828 (to which it keys out in the paper by Cole *et al.* 2013) and *Apostolepis* Cope, 1862. In the field, *Paikwaophis* is easily distinguished from *Atractus* (assigned to the subfamily Dipsadinae; Zaher 1999) by the absence of a loreal (present in *Atractus*; e.g. Hoogmoed 1980, Kok 2006) and two pairs of chinshields (single pair in *Atractus*; e.g. Hoogmoed 1980, Kok 2006); and from *Apostolepis* (assigned to the tribe Elapomorphini; see Zaher *et al.* 2009) by having 17 dorsal scale rows (15 in *Apostolepis*; e.g. Entiauspe-Neto *et al.* 2021) and paired nasals (nasal plate undivided in *Apostolepis*; e.g. Entiauspe-Neto *et al.* 2021). It should be stressed that outside the family Dipsadidae, *Paikwaophis* could possibly be confused with the colubrid genus *Tantilla* Baird and Girard, 1853, from which it is distinguished immediately by having 17 dorsal scale rows (15 in *Tantilla*; e.g. Koch and Venegas 2016).

Content: Currently monotypic, containing only *Paikwaophis kruki*.

Distribution: Known only from the type locality (see 'Holotype' below).

Paikwaophis kruki gen. nov., sp. nov.

Zoobank registration: urn:lsid:zoobank.org:act:A7918471-9399-4AEA-AD08-D176E13D53ED

Holotype: RBINS 2734 (field number CPI11310; Figs 4–13), an immature female, collected by D. Bruce Means on 24 February 2021 at 'Sloth Camp' [5.247074° N, 60.705471° W; ~1180 m elevation; Cuyuni-Mazaruni District (Region 7), Guyana, South America], which is located on a broad ridge running downhill along the west fork of the Paikwa River from the bottom of the talus slope below the vertical cliff wall of Wei-Assipu-tepui (Fig. 2).

Etymology: The specific epithet '*kruki*' is a noun in the genitive case, honouring Professor Andrzej Kruk (born 1971), the current Dean of the Faculty of Biology and Environmental Protection at the University of Łódź, Poland, for his friendship and his influential contribution in enhancing the quality of research at the University of Łódź.

Diagnosis: The species diagnosis is the same as for the genus.

Description of holotype: The specimen is a small immature female (Figs 4–13), with TL 180 mm, TaL 24 mm (13% of TL);

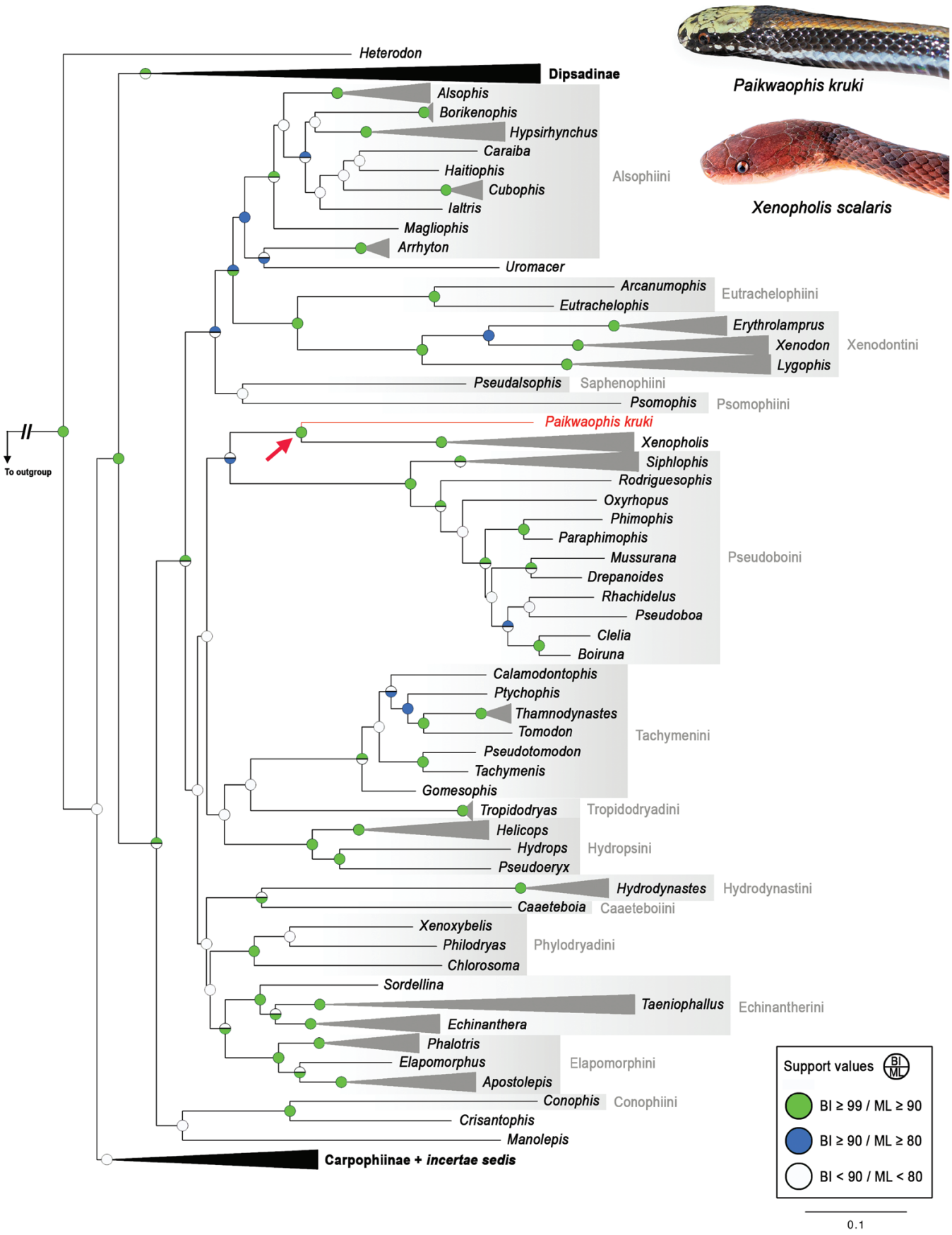

Figure 3. Phylogenetic relationships of the family Dipsadidae inferred from a concatenated dataset of six genes (four mtDNA and two nuDNA genes; 3772 bp) using Bayesian inference. Statistical supports for both Bayesian and maximum likelihood (IQ-TREE) analyses are provided at nodes (see key, lower right inset). Photographs are by D.B.M. (***Paikwaophis kruki***) and courtesy of the Reptiles of Ecuador book project (*Xenopholis scalaris*).

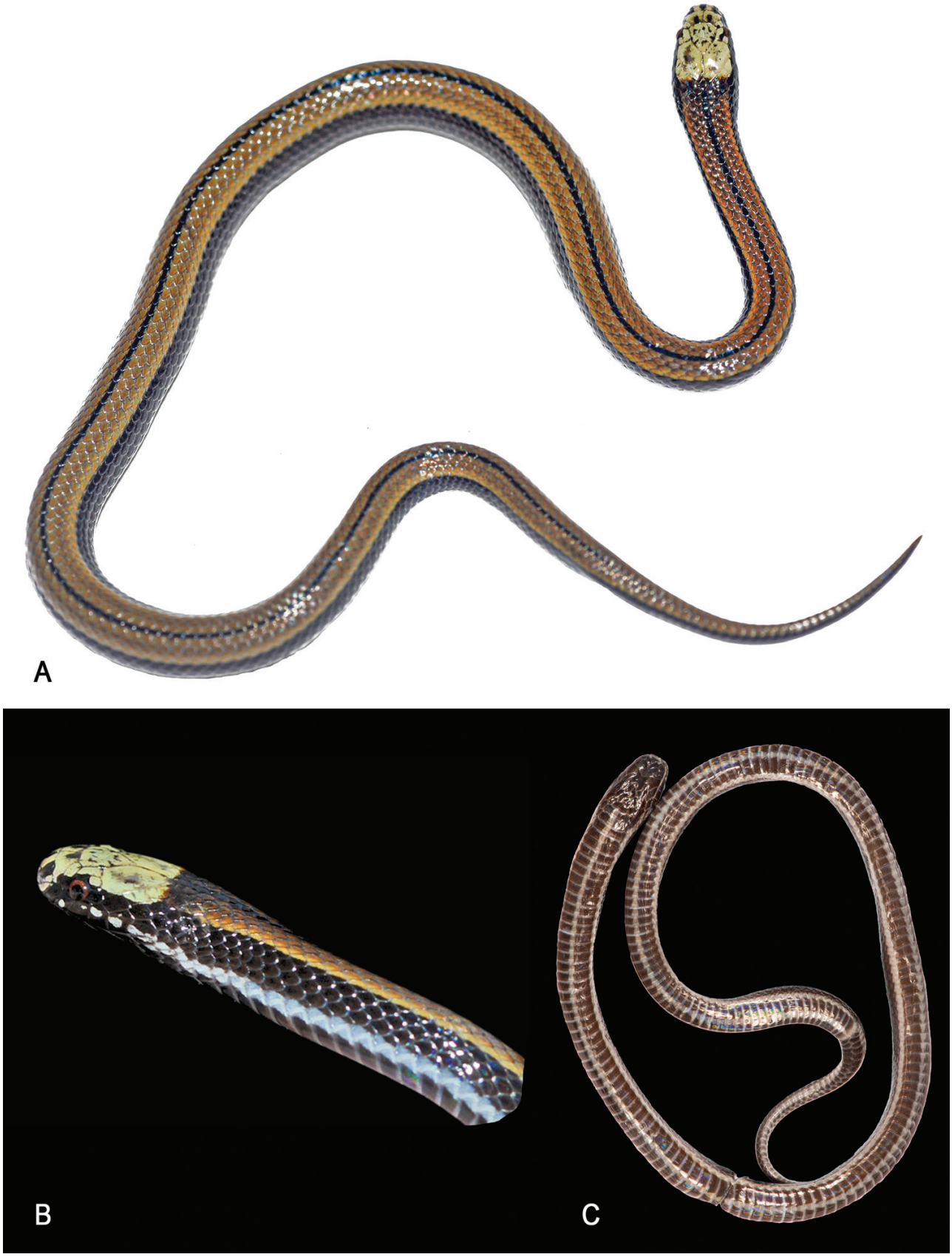

Figure 4. Holotype of ***Paikwaophis kruki*** (*RBINS 2734*). A, dorsal view in life (photograph by D.B.M.). B, dorsolateral view of anterior body in life (photograph by D.B.M.). C, ventral view in preservative (photograph by P.J.R.K.).

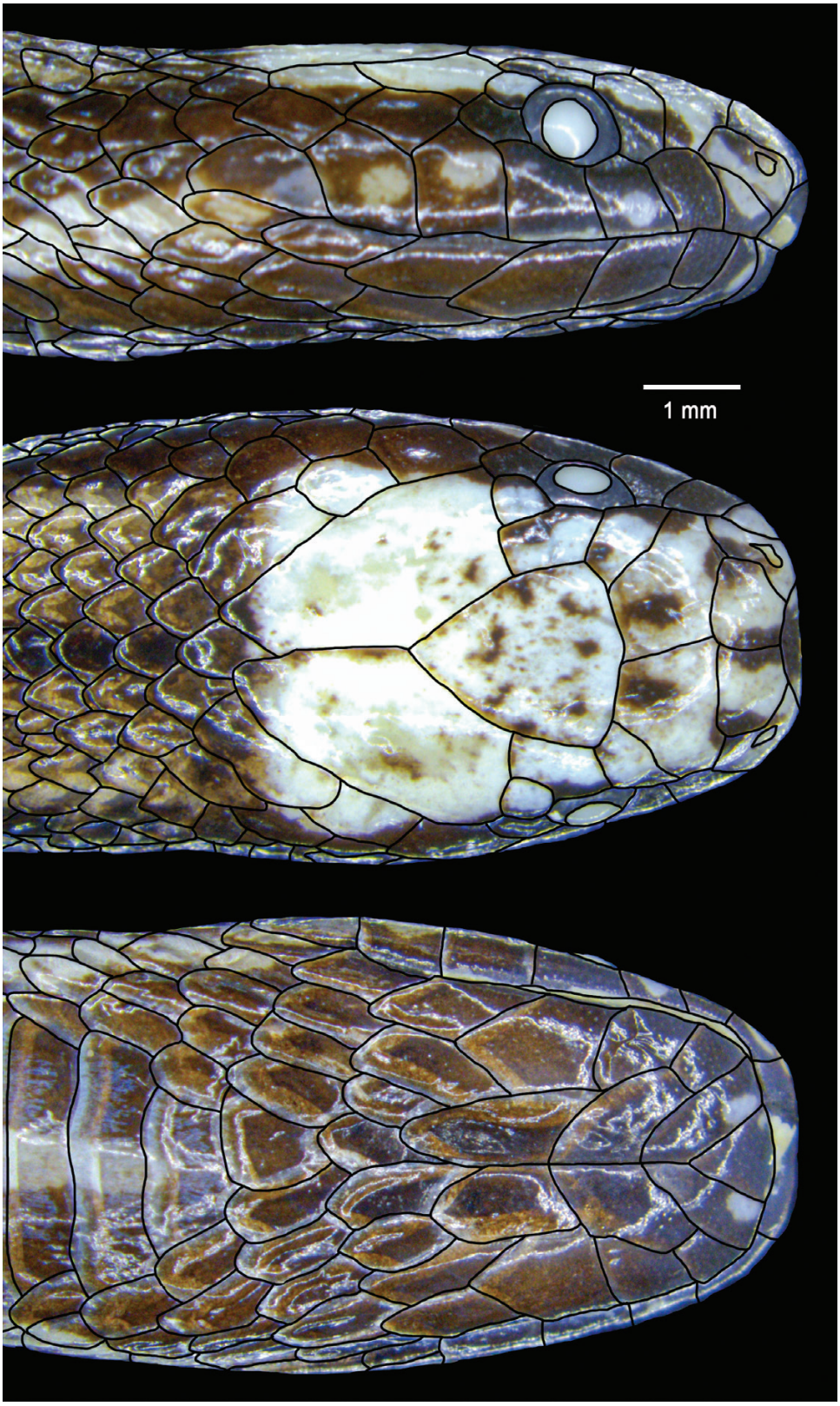

Figure 5. Pholidosis of the head of the holotype of ***Paikwaophis kruki*** (*RBINS 2734*) (photographs by P.J.R.K.).

HL 7.1 mm (4% of TL); HW 4.7 mm (66% of HL); snout short and blunt, SnL 2.1 mm (30% of HL); ED 1.0 mm; DSN 0.6 mm; and DNE 1.5 mm. Head poorly distinct from neck; body robust, slightly wider than high. Dorsal scales rhomboid, smooth, lacking keels or apical pits, DSR 17-17-17. There are 171 ventrals, an undivided anal scale and 38 paired subcaudals.

Figure 6. Three-dimensional model of the complete skeleton of the holotype of ***Paikwaophis kruki*** (*RBINS 2734*) based on µCT imagery. A, dorsal view. B, ventral view.

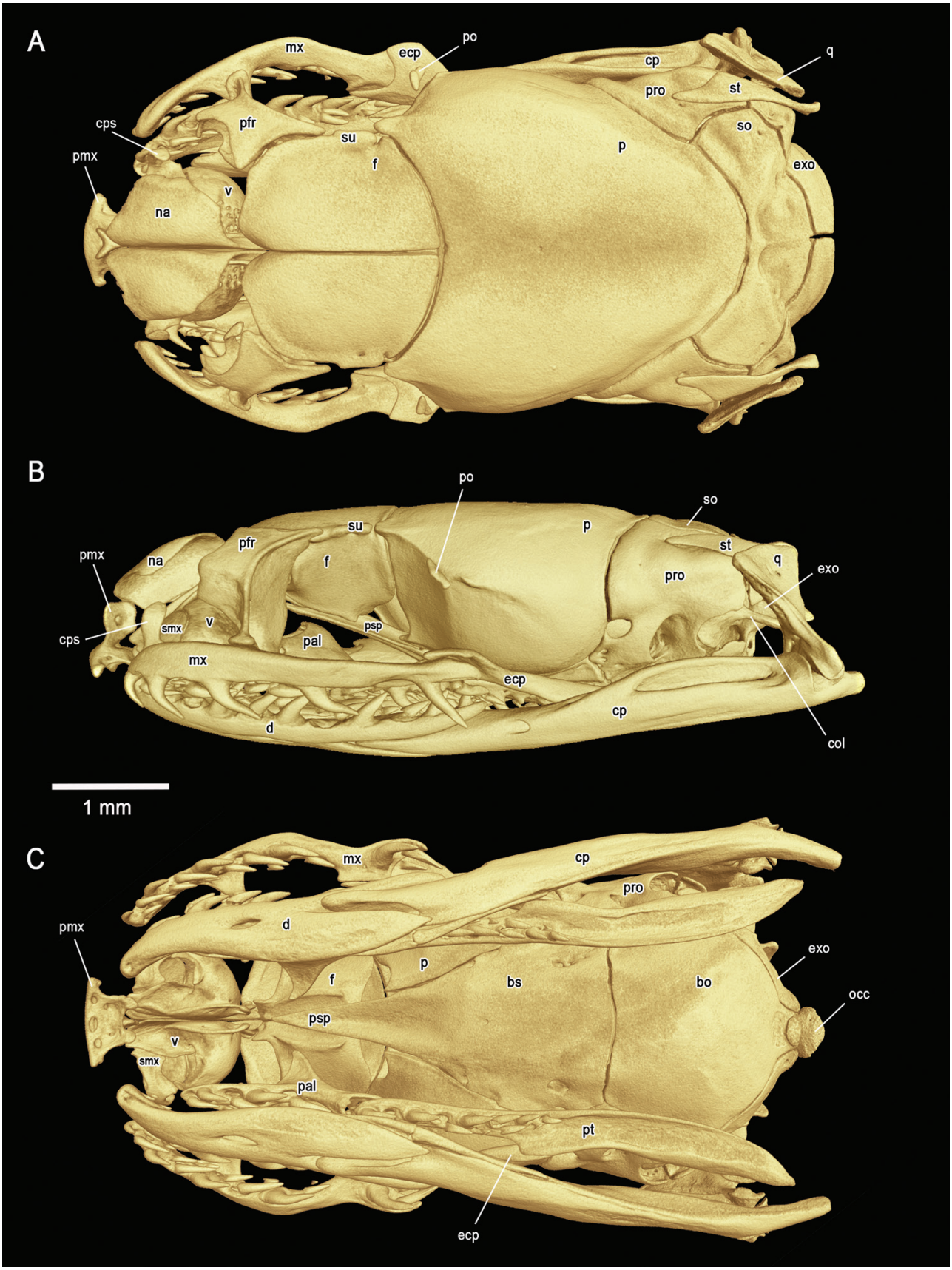

Figure 7. Three-dimensional model of the skull of the holotype of ***Paikwaophis kruki*** (*RBINS 2734*) based on µCT imagery. A, dorsal view. B, lateral view. C, ventral view. Abbreviations: bo, basioccipital; bs, basisphenoid; col, columella; cp, compound bone; cps, conchal process of septomaxilla; d, dentary; ecp, ectopterygoid; exo, exoccipital; f, frontal; mx, maxillary; na, nasal; occ, occipital; p, parietal; pal, palatine; pfr, prefrontal; pmx, premaxilla; po, postorbital; pro, prootic; psp, parasphenoid rostrum; pt, pterygoid; q, quadrate; smx, septomaxilla; so, supraoccipital; st, supratemporal; su, supraorbital; v, vomer.

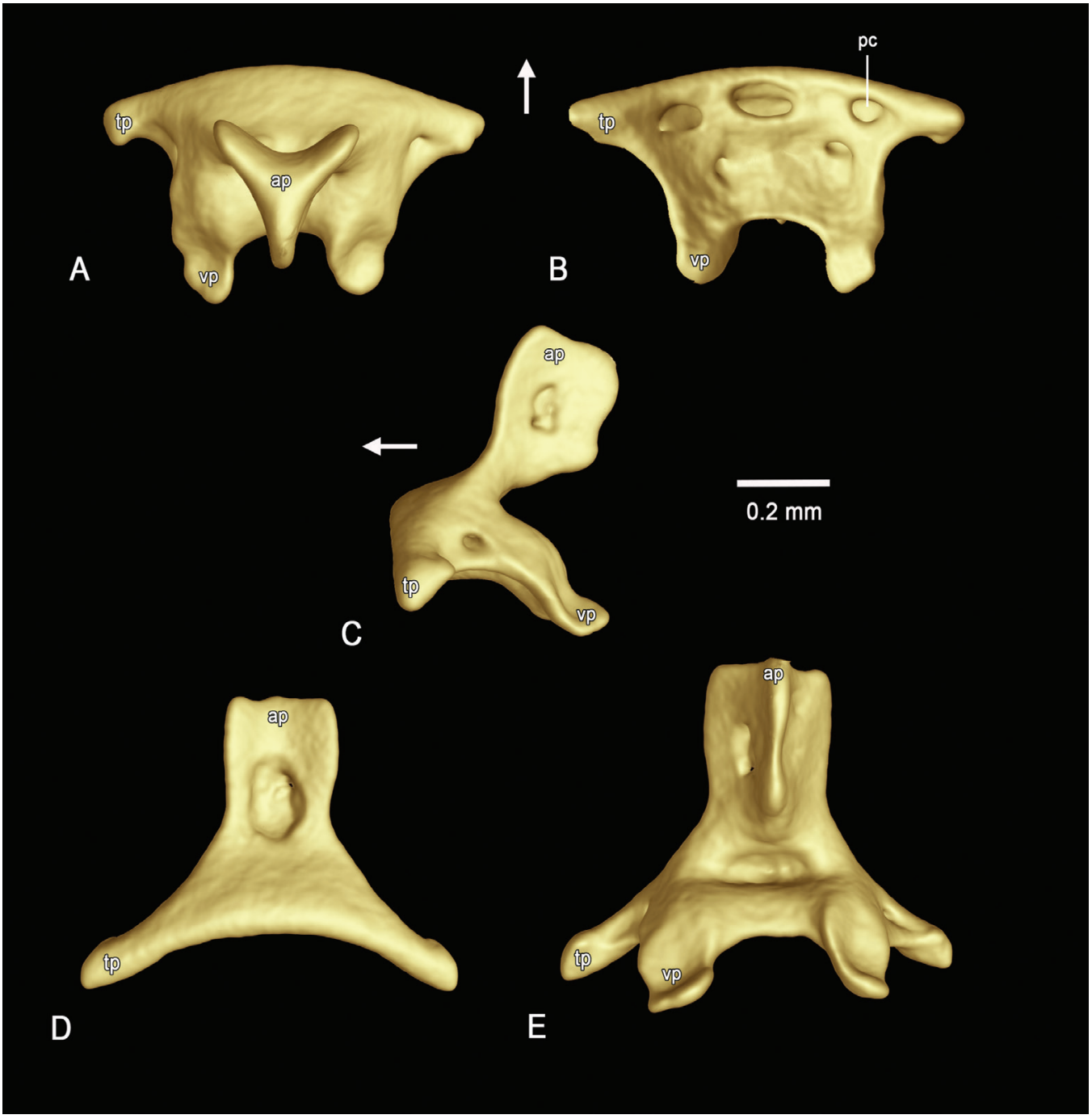

Figure 8. Three-dimensional model of the premaxilla of the holotype of ***Paikwaophis kruki*** (*RBINS 2734*) based on μCT imagery. A, dorsal view. B, ventral view. C, lateral view. D, anterior view. E, posterior view. Abbreviations: ap, ascending process of premaxilla; pc, premaxillary channel; tp, transverse process of premaxilla; vp, vomerine process of premaxilla. The white arrows point to the rostral end of the cranium.

Dentition diacranterian, aglyphous opisthodont. Prediastemal maxillary teeth 7, postdiastemal teeth 2.

Rostral 3.6 times wider than high (RW 1.8 mm, RH 0.5 mm), visible from above, contacting first supralabials, nasals and internasals. Paired internasals 1.3 times wider than long, laterally in contact with nasals. Paired prefrontals large, 1.5 times broader than long, laterally contacting nasals, second supralabials and preoculars. Frontal subtriangular, anteriorly convex, with dorsal termination acute, ~1.2 times longer than wide, laterally in contact with supraoculars, laterodorsally in contact with parietals. Elongate single supraocular ~2 times longer than wide. Parietals large, ~2 times longer than wide, median suture ~1.5 times shorter than frontal length. Nostrils located in anterior portion of undivided nasals, which are 2 times longer than high. Nasals in contact with rostral, internasals, first and second supralabials and prefrontals. Loreal absent, seemingly fused with prefrontal. Eyes moderate in size, with vertically oval pupils, poorly visible in

Figure 9. Three-dimensional model of the left maxilla of the holotype of ***Paikwaophis kruki*** (*RBINS 2734*) based on µCT imagery. A, labial view. B, lingual view. C, dorsal view. D, ventral view. Abbreviations: ep, ectopterygoid process; pp, palatine process. The white arrows point to the rostral end of the cranium.

ventral view, surrounded by one preocular, one supraocular, two postoculars and third and fourth supralabials. No subocular. Preocular ~2 times higher than long. Supralabials 7/7, with numerous minute sensory pits, irregularly increasing in size posteriorly; last one ~2 times longer, but as high as first; second supralabial contacting nasal, prefrontal and preocular; third contacting preocular and eye; fourth contacting eye and lower postocular; fifth contacting lower postocular and anterior temporal; sixth contacting anterior and lower posterior temporals; seventh contacting lower posterior temporal and first scale of dorsolateral and lateral body scale row. Temporals 1 + 2 + 3; first and second temporals about twice as long as high; third temporals almost as long as high. Mental triangular, as long as wide, separated from chinshields by first pair of infralabials, which are in contact with each other along the ventral midline. Infralabials 7/7, with numerous minute sensory pits; fourth the largest, second the smallest; first to fourth contacting anterior pair of chinshields (fourth in point contact); fourth infralabial contacting posterior chinshield and first gular. Two pairs of chinshields; anterior chinshields projecting frontolaterally, about twice as wide as long and ~1.6 times shorter than posterior chinshields; posterior chinshields ~2.5 times longer than wide, laterally contacting fourth infralabial, posteriorly separated from first preventral by two rows of gulars. Anterior row of gulars consists of six scales; second row consists of seven scales.

Summary of morphometric and meristic data: SVL 156 mm; TaL 24 mm; TL 180 mm; HL 7.1 mm; HW 4.7 mm; ED 1.0 mm; DSN 0.6 mm; DNE 1.5 mm; SnL 2.1 mm; RW 1.8 mm; RH 0.5 mm; DSR 17-17-17; SL 7/7; IL 7/7; PrO 1; PtO 2; SuO 1; IN 2; LoR 0; TMP 1 + 2 + 3; CS 2 + 2; V 171; SC 38.

Coloration of holotype in life (Fig. 4A, B): The top of the head is boldly marked with a dense light yellowish cream colour from the rounded tip of the snout distally to the ends of the parietal shields, and laterally ending abruptly where the top of the head makes a sharp downturn to the vertical sides of the face. Dense black pigment surrounds the nostrils, completely colouring the small rostral, and makes two similar-sized black spots at the distal edges of the prefrontals. Small black specks are scattered loosely on the frontal and parietal scales and in some of the depressions between the head scales. The sides of the face are coal black beginning on the loreal and anterior-most labial in front of the eye and sweeping backwards from the orbit to become a two- to three-scale-wide dorsolateral intense black stripe all the

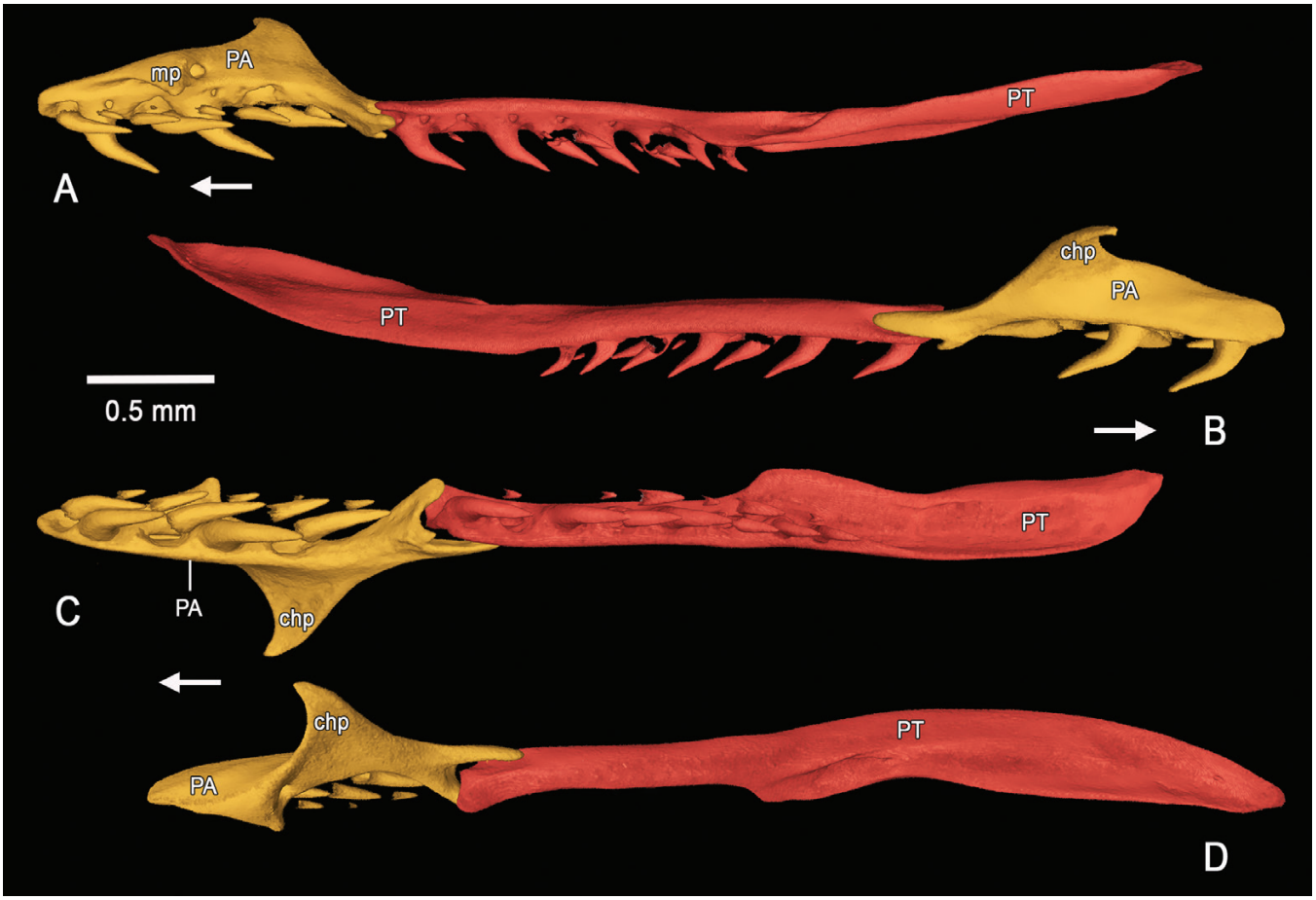

Figure 10. Three-dimensional model of the left palatine and pterygoid of the holotype of ***Paikwaophis kruki*** (*RBINS 2734*) based on µCT imagery. A, labial view. B, lingual view. C, ventral view. D, dorsal view. Abbreviations: chp, choanal process of the palatine; mp, maxillary process of palatine; PA, palatine; PT, pterygoid. The white arrows point to the rostral end of the cranium.

way onto the tail. The eye is entirely embedded in the black lateral stripe. The iris is dark reddish orange or rust coloured. Also beginning on the upper labials are three or four light blue spots that fuse posteriorly and become a very distinct ventrolateral stripe including the ventral-most dorsal scale and a small lateral-most portion of the adjacent ventral scales, running in parallel with the wider black stripe all the way onto the sides of the tail. The ventral pattern is a shiny, slick black colour beginning at the base of the chin and running all the way to the tip of the tail. A bold white to very light blue midventral stripe about one-fifth the width of the black ventral scales begins on the second ventral scale and runs all the way to the anal scale. The undersurface of the chin is densely black, but the chinshields have small whitish blotches, and each lower labial has a bold white oval spot. The dorsal pattern consists of a thin, one-scale-wide, continuous, black line in the middle of an eight- or nine-scale light brown stripe. The main impressions of the colour pattern are a light brown snake with a boldly whitish head and a light bluish streak on dense black sides.

Coloration of the holotype in preservative (Fig. 4C, 5): After 22 months in ethanol preservative, the overall coloration of the holotype appears only slightly faded from the condition of the live snake. The light brown dorsal colour has faded slightly, but the black-pigmented venter, lateral and middorsal stripes and chin are essentially the same. The blue colour of the lateral and midventral stripes has disappeared from the remaining underlying white colour.

Osteology (Figs 6–13): Skull and postcranial skeleton are well ossified.

Snout: The premaxilla (Fig. 8) is short and blunt. The ascending process is frontolaterally expanded and slanted posteriorly, giving it a wishbone shape from above, with its anterior surface having a sigmoid curvature in the lateral view. The transverse process is short and slightly curved, almost rectangular in shape in dorsal view. The posterior end of the vomerine process bears a notch; it fails to contact the tip of the septomaxilla. Both anterior and posterior sections of the nasal bone are tapered; the dorsal surface is bulged.

Braincase (Fig. 7): The parietal is short and blunt, lacking a conspicuous lateral ridge (= adductor ridge). The lateral aspect of the prefrontal exhibits an expanded lateral lamina. The dorsal margin of the prefrontal bears a notch that almost contacts the lateral edge of the dorsal lamina of the nasal. The lateral aspect of the prefrontal shows a conspicuous outer orbital ridge. The lateral foot process is well developed, in contact with the dorsal surface of the maxilla, where it expands

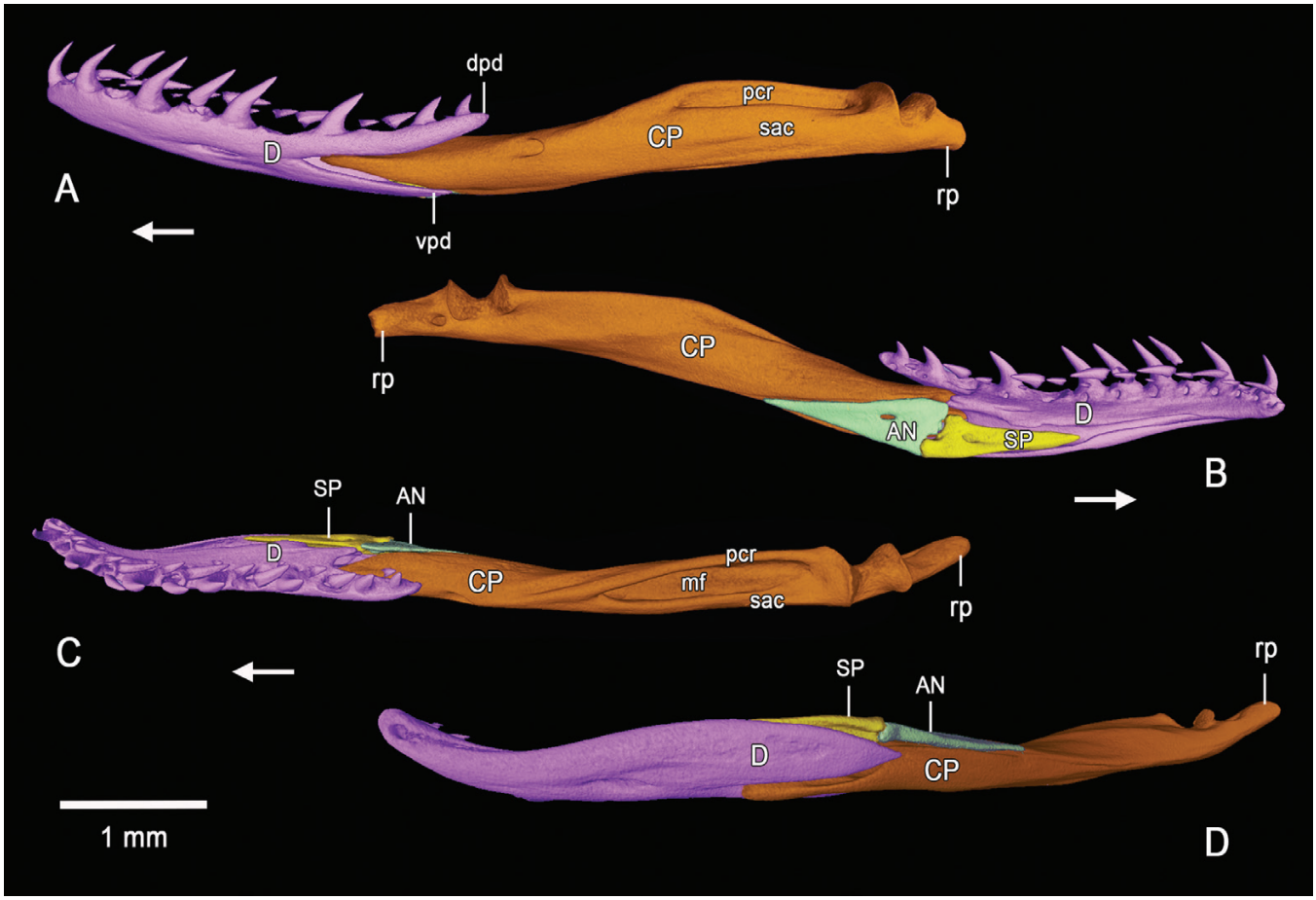

Figure 11. Three-dimensional model of the left mandible of the holotype of ***Paikwaophis kruki*** (*RBINS 2734*) based on μCT imagery. A, labial view. B, lingual view. C, dorsal view. D, ventral view. Abbreviations: AN, angular; CP, compound bone; D, dentary; dpd, dorsal process of dentary; mf, mandibular fossa; pcr, prearticular crest; rp, retroarticular process of compound bone; sac, surangular crest of compound bone; SP, splenial; vpd, ventral process of dentary. The white arrows point to the rostral end of the cranium.

frontally and dorsally as a plate, giving it an inverted T-shape in lateral view. The medial extension is short, poorly differentiated and almost in contact with the pterygoid. The lacrimal foramen is large and vertically ovoid. The anterior margin of the frontal is trapezium-shaped; the lateral margin is slightly convex. The postorbital is highly reduced, crescent-shaped, not in contact with the frontal. Supraoccipital sagittal and adductor crests are poorly developed. The basisphenoid is wide, with no conspicuous lateral ridges on the ventral surface. The parasphenoid rostrum is not divided. The columella is short and thick, approximately as long as the diameter of its footplate.

Palatomaxillary arch: The maxilla (Fig. 9) is short and stout, with a strong sigmoid curvature in dorsal and ventral view. The palatine process of the maxilla is elongate, with its tapered rounded tip strongly curved towards the ectopterygoid process. The ectopterygoid process is expanded, short and sharp. The maxilla has nine teeth on each side, with one row of replacement teeth on the lingual side. The palatine (Fig. 10) bears five teeth, with one row of replacement teeth on the labial side. The choanal process of the palatine is curved towards the rostral end of the cranium and is shark-fin-shaped in dorsal view. The maxillary process of the palatine is short and small. The pterygoid (Fig. 10) is slender and lanceolate, ~1.6 times the length of the palatine, bearing eight teeth on its anterior portion only (i.e. approximately half of its length), with one row of replacement teeth on the labial side. The ectopterygoid process is large and well defined, outwardly curved in dorsal view; its anterior part is horizontally expanded, bearing a large notch. The lateral furculum of the ectopterygoid is short and sharp; the medial furculum is straight and elongate with a pointed tip.

Suspensorium and mandible: The mandible (Fig. 11) is stout and moderately curved. The dorsal process of the dentary is upwardly curved and expands further posteriorly than the ventral process. The dentary bone bears 12 teeth, with one row of replacement teeth on the lingual side. The largest dentary nutrient foramen is elongated, oval-shaped and lies below the seventh tooth. The prearticular crest of the compound bone is about twice as high as the surangular crest. The angular is slender and triangular. The splenial is triangular, tooth-shaped and slightly shorter than the angular. The supratemporal is flat and slender, having a sigmoid curvature in the dorsal view, with its posterior margin outwardly curved. The quadrate is expanded and stout, almost triangular in lateral view, and approximately as long as the supratemporal. The supratemporal angular surface of the quadrate is expanded and elongated. The

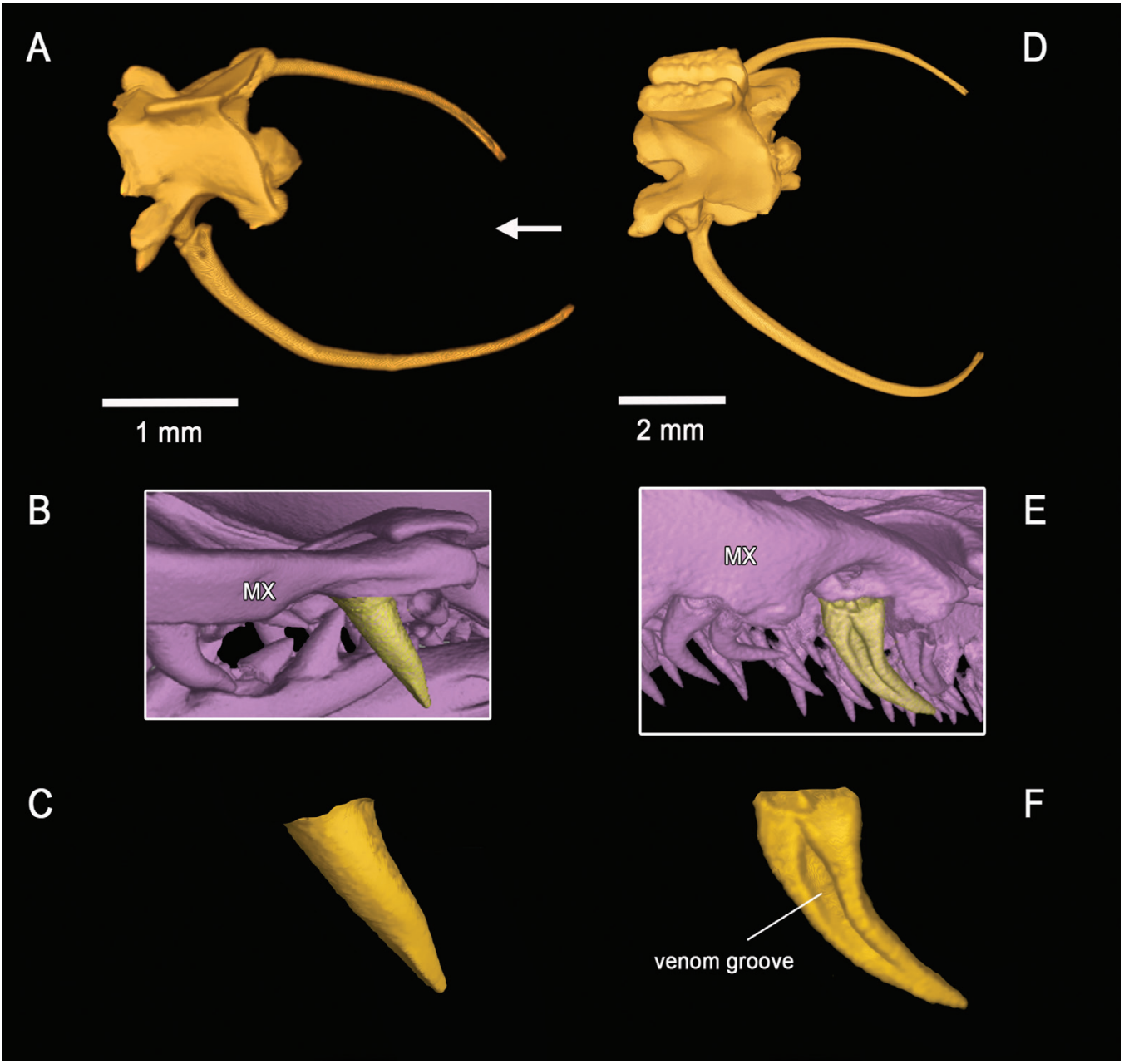

Figure 12. A, D, three-dimensional model of a mid-body vertebra of: A, the holotype of ***Paikwaophis kruki*** (*RBINS 2734*); and D, *Xenopholis scalaris* (NHMUK 2023.3195) based on µCT imagery. B, C, E, F, three-dimensional model of the last maxillary tooth of: (B, C) the holotype of ***Paikwaophis kruki*** (*RBINS 2734*); and (E, F) *X. scalaris* (NHMUK 2023.3195) based on µCT imagery. Abbreviation: MX, maxillary. The white arrow points to the rostral end of the cranium.

stylohyal is long, completely fused with the quadrate, strongly protruding backwards.

Dentition: Diacranterian (presence of a diastema), aglyphous opisthodont (ungrooved fangs); prediastemal maxillary teeth: 7/7; postdiastemal maxillary teeth: 2/2; pterygoid teeth: 8/8; palatine teeth: 5/5; dentary teeth: 12/12.

Postcranial skeleton: Trunk vertebrae 175, neural spines smooth, ungrooved and not laterally expanded; conspicuous hypapophyses present on anterior trunk vertebrae only (approximately one-quarter of trunk vertebrae, hypapophyses abruptly decreasing in size from ~46th vertebra), absent on posterior vertebrae; caudal vertebrae 42, with distinct haemapophyses.

Distribution and natural history: The forest at the type locality is a fairly dense growth of small [10–13 cm diameter at breast height (DBH)] to medium (15–45 cm DBH) trees, with an occasional large tree > 45 cm DBH. Their trunks are densely grown, with a 5-cm-deep cover of moss to ≥ 1.5 m above the ground, but many trees are mossy to their canopy limbs. The trees are ~30 m high, and few have branches until ~25 m. Large aroids with big whorled leaves are epiphytes from ground level to the bottom

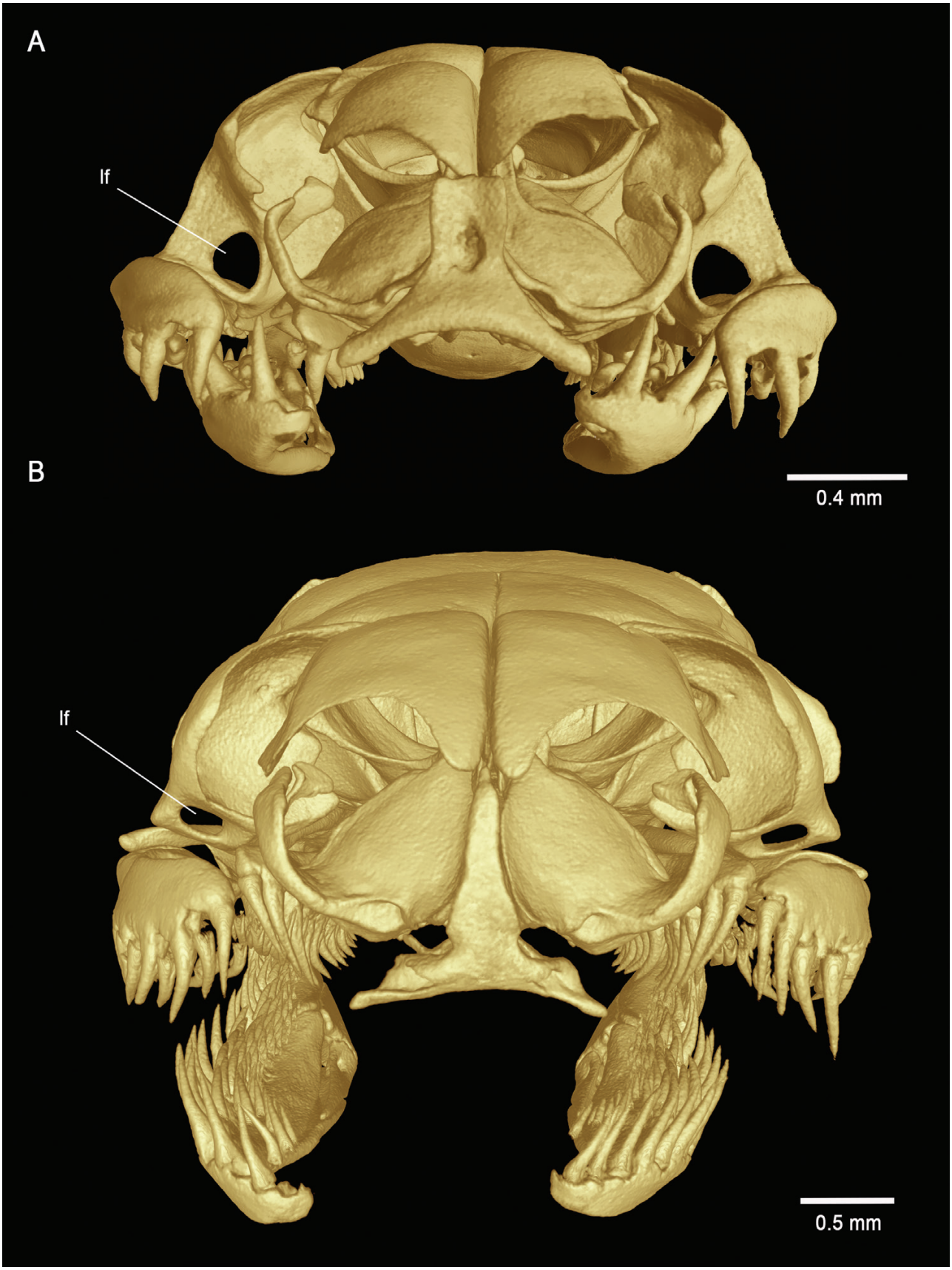

Figure 13. Three-dimensional model of the skull of: A, the holotype of ***Paikwaophis kruki*** (*RBINS 2734*); and B, *Xenopholis scalaris* (NHMUK 2023.3195) in frontal view, based on μCT imagery. Abbreviation: lf, lacrimal foramen.

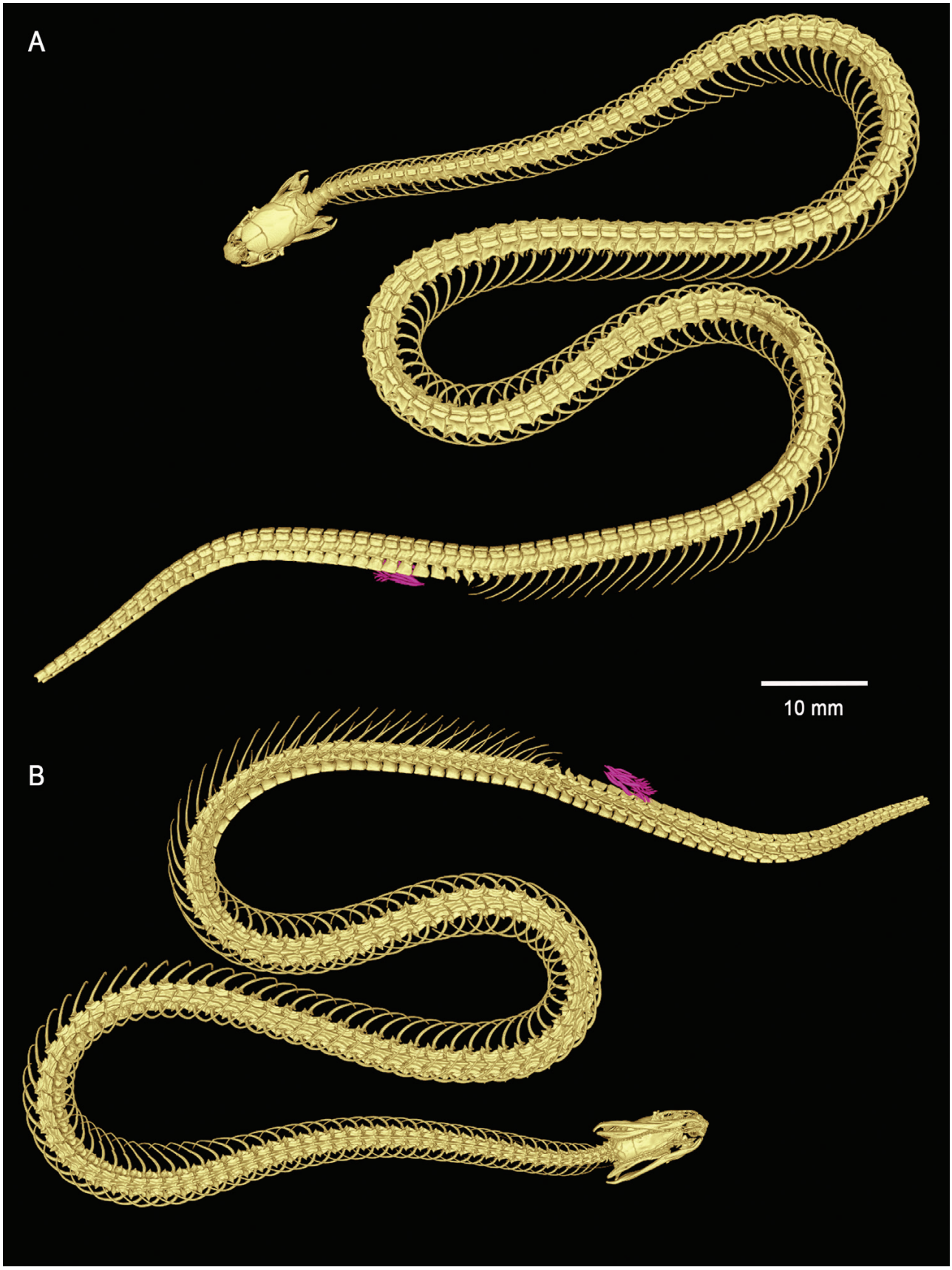

Figure 14. Three-dimensional model of the complete skeleton of the syntype of *Xenopholis scalaris* (BMNH 1946.1.8.66) based on μCT imagery. A, dorsal view. B, ventral view. Note the hemipenial body in pink.

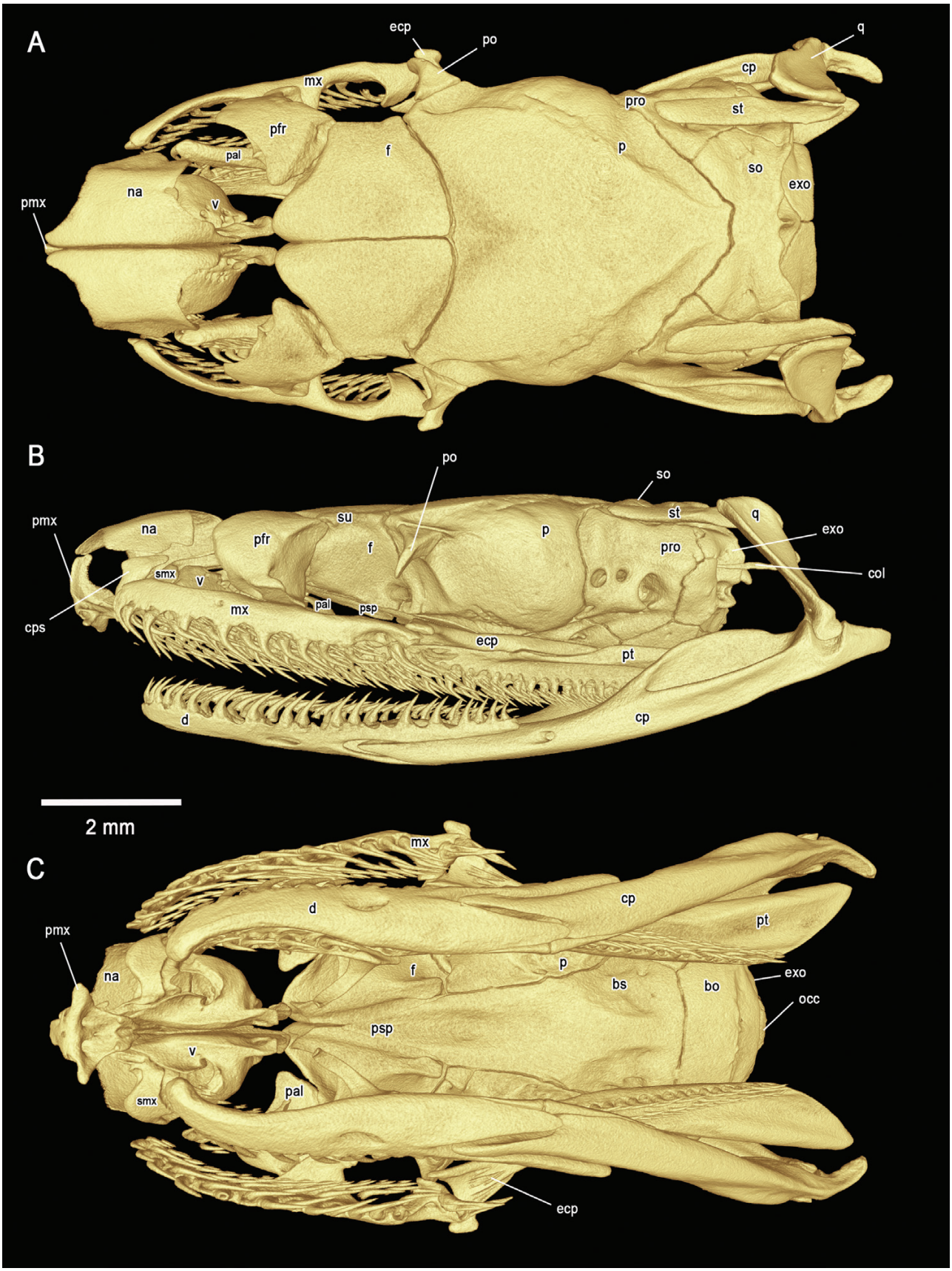

Figure 15. Three-dimensional model of the skull of *Xenopholis scalaris* (NHMUK 2023.3195) based on µCT imagery. A, dorsal view. B, lateral view. C, ventral view. Abbreviations: bo = basioccipital; bs, basisphenoid; col, columella; cp, compound bone; cps, conchal process of septomaxilla; d, dentary; ecp, ectopterygoid; exo, exoccipital; f, frontal; mx, maxillary; na, nasal; occ, occipital; p, parietal; pal, palatine; pfr, prefrontal; pmx, premaxilla; po, postorbital; pro, prootic; psp, parasphenoid rostrum; pt, pterygoid; q, quadrate; smx, septomaxilla; so, supraoccipital; st, supratemporal; su, supraorbital; v, vomer.

of the canopy branches, but only on ~20% or less of the trees. An understorey layer of small-diameter brush with dwarf palms and long, strap-leaved Rapateaceae exists, with lots of pesky vines that make walking a challenge. The ground is covered with 30–45 cm of recently fallen leaf litter over peaty soil invaded by fine roots growing upwards from larger roots of the trees. Many of the small- to medium-sized trees are prop-rooted species, with a labyrinth of declivities among them filled with leaf litter and/or moss. These are havens for many tiny frogs that we hear calling all day long and at night. The mossy epiphyte load is not so vigorous as in a more substantial cloud forest, but getting there.

The skull of *Paikwaophis kruki* appears to be conducive to burrowing in the soft peaty soil immediately under the decomposing top layer of the leaf litter of cloud forests, and we assume that the new genus is fossorial or semi-fossorial, as also suggested by, inter alia, the highly reduced postorbital bones (Cundall and Irish 2008).

Paikwaophis kruki is saurophagous, at least in part, given that we found a few small lizard scales in the large intestine of the holotype.

Unlike its sister genus (*Xenopholis*), defensive mechanisms, such as body flattening and head hiding (e.g. Mira-Mendes *et al.* 2013, de Oliveira Meneses *et al.* 2022), have not been observed in *Paikwaophis*.

DISCUSSION

Molecular data strongly support *Paikwaophis* to be a member of Xenodontinae (Dipsadidae), most closely related to the genus *Xenopholis*. The sister relationship with *Xenopholis* is surprising because these two genera are strikingly different both morphologically and osteologically. Given that the holotype of *Paikwaophis* is an immature female, we used only comparative osteological characters that are not strongly influenced by ontogenetic changes (e.g. dentition and shape of vertebrae; see Palci *et al.* 2016, for instance). Although a lack of material hampers a thorough osteological comparative analysis with all known Xenodontinae genera, our results suggest that homoplasy is widespread in osteological characters in this group and could confound evolutionary inferences; a finding that is consistent with the results of, e.g. Hofstadler-Deiques and Lema (2005), who inferred close phylogenetic affinities between Elapomorphini and Atractaspididae based on cranial morphology, an assumption unsupported by any recent comprehensive molecular phylogenetic analyses (e.g. Pyron *et al.* 2011).

Our results provide new insights on the molecular phylogenetic position of *Xenopholis*, a genus until now considered as *incertae sedis* based on both morphology (e.g. Zaher 1999, Jansen *et al.* 2009) and molecular data (e.g. Grazziotin *et al.* 2012, Pyron *et al.* 2011, 2015). Recent molecular phylogenies placed *Xenopholis* either sister to *Hydrodynastes* Fitzinger, 1843 (e.g. Pyron *et al.* 2011, 2015, Grazziotin *et al.* 2012) or to Caaeteboiini (Moraes *et al.* 2021), all with low support. Given that no data about hemipenial characters are available for *Paikwaophis* at this stage, we refrain from erecting two new distinct tribes for *Xenopholis* and *Paikwaophis*, but we note that the recognition of higher taxa for these two genera could be appropriate.

It should be mentioned that the syntype of *X. scalaris* in NHM is BMNH 1946.1.8.66 and not BMNH 1946.1.8.60 as reported in the literature and most online databases since Peters (1960).

CONCLUSION

Paikwaophis kruki is a rare species of aglyphous dipsadid, known only from the recently collected female holotype and probably restricted to the cloud forest of the Eastern Pantepui District in the Guiana Shield highlands. Its closest known relative is the genus *Xenopholis*, an opisthoglyphous Xenodontinae characterized by unique and distinctive vertebrae (neural spines expanded laterally, forming rugose shields divided by a median groove). *Xenopholis* is widespread in South America and currently contains three species. The two genera are strikingly different both morphologically and osteologically. The skeletal morphology of *Paikwaophis kruki* suggests that it is fossorial or semi-fossorial, which could help to explain its apparent rarity. This description brings the number of Pantepui endemic reptile genera to six. To date, *Paikwaophis* is the only known endemic snake genus in the Pantepui biogeographical region.

SUPPLEMENTARY DATA

Supplementary data is available at *Zoological Journal of the Linnean Society* online.

ACKNOWLEDGEMENTS

For logistical support and assistance in the field we thank Tony Thorne, Claire Antell, Delice Rogers, Wally Prince and Leon Moore of Wilderness Explorers Guyana. D.B.M. thanks National Geographic expedition members who helped him: Mark Synnott, Alex Honnold, Federico Pisani, Brian Irwin, Renan Ozturk, Taylor Rees, Ryan Valasek, Matthew Irving and Rudy Lehfeldt-Ehlinger. We are also grateful to all the citizens of the village of Phillipai for their assistance, ensuring that the Wei-Assipu Expedition was successful, and for their friendship. We thank Patrick Campbell (NHM), Jeff Streicher (NHM) and Mark Wilkinson (NHM) for access to museum specimens under their care and constructive discussions. We thank Brett Clark (NHM) for technical assistance in µCT scanning. Research (020821BR003) and export (Material Transfer Agreement EPAMTA020821BR003) permits were issued by the Guyana Environmental Protection Agency. We thank Jeff Streicher (NHM) and an anonymous reviewer for helpful suggestions.

Conflict of interest: none declared.

FUNDING

This research was supported by a Marie Skłodowska-Curie Actions (MSCA) grant (101022238/HOSTILE) to P.J.R.K. The expedition to film the documentary *Explorer, The Last Tepui* was funded by the National Geographic Society.

DATA AVAILABILITY

The data underlying this article are available in the GenBank Nucleotide Database at https://www.ncbi.nlm.nih.gov, where they can be accessed with accession numbers OR069380–OR069383, OR075146 and OR075194, and on the MorphoSource platform at https://www.morphosource.org/projects/000523050.

REFERENCES

Amaral A. Collecta herpetologica no nordeste do Brasil. *Memórias do Instituto Butantan* 1935 [1934];**8**:185–94.

Arredondo JC, Grazziotin FG, Scrocchi GJ *et al*. Molecular phylogeny of the tribe Philodryadini Cope, 1886 (Dipsadidae: Xenodontinae): rediscovering the diversity of the South American Racers. *Papéis Avulsos de Zoologia* 2020;**60**:e20206053.

Berry PE, Huber O, Holst BK. Floristic analysis and phytogeography. In: Berry PE, Holst BK, Yatskievych K (eds.), *Flora of the Venezuelan Guayana. Vol. 1. Introduction*. St Louis: Missouri Botanical Garden Press, 1995, 161–92.

Boulenger GA. Description of a new batrachian (*Oreophryne quelchii*) discovered by Messrs. J. J. Quelch and F. McConnell on the summit of Mount Roraima. *Annals and Magazine of Natural History* 1895;**6**:521–2.

Briceño HO, Schubert C. Geomorphology of the Gran Sabana, Guayana Shield, southeastern Venezuela. *Geomorphology* 1990;**3**:125–41.

Campbell JA, Smith EN, Hall AS. Caudals and calyces: the curious case of a consumed Chiapan colubroid. *Journal of Herpetology* 2018;**52**:458–71.

Cole CJ, Townsend CR, Reynolds RP *et al*. Amphibians and reptiles of Guyana, South America: illustrated keys, annotated species accounts and a biogeographic synopsis. *Proceedings of the Biological Society of Washington* 2013;**125**:317–578.

Cundall D, Irish FJ. The snake skull. In: Gans C, Gaunt AS, Adler K (eds.), *The Skull of Lepidosauria*. Ithaca: Society for the Study of Amphibians and Reptiles, 2008, 349–692.

Cunha OR, Nascimento FP. Ofídios da Amazônia. XVI - A especie *Uromacerina ricardini* (Peracca, 1897) na Amazônia oriental (Leste do Pará) (Ophidia: Colubridae). *Boletim do Museu Paraense Emílio Goeldi Zoologia. Belem* 1982;**113**:1–9.

Davis SD, Heywood VH, Hamilton A. *Centres of Plant Diversity: a Guide and Strategy for their Conservation, Vol. 3, The Americas*. Cambridge: IUCN Publications Unit, 1997.

de Oliveira Meneses AS, Fernandes M, Torres Cardoso AG *et al*. Esconder la cabeza en *Xenopholis undulatus* (Dipsadidae) en el Brasil central. *Revista Latinoamericana de Herpetología* 2022;**5**:194–6.

Dowling HG. A proposed standard system of counting ventrals in snakes. *British Journal of Herpetology* 1951;**1**:97–9.

Doyle AC. *The Lost World, being an account of the recent amazing adventures of Professor George E. Challenger, Lord John Roxton, Professor Summerlee, and Mr. E. D. Malone of the 'Daily Gazette'*. London: Hodder and Stoughton, 1912.

Entiauspe-Neto OM, Koch C, Harvey MB *et al*. Redescription of *Apostolepis ambiniger* (Peters, 1869) (Serpentes: Dipsadidae: Elapomorphini). *Vertebrate Zoology* 2021;**71**:231–51.

Faivovich J, Haddad CFB, Garcia PCA *et al*. Systematic review of the frog family Hylidae, with special reference to Hylinae: phylogenetic analysis and taxonomic revision. *Bulletin of the American Museum of Natural History* 2005;**294**:1–240.

Forstner MRJ, Davis SK, Arevalo E. Support for the hypothesis of Anguimorph ancestry for the suborder Serpentes from phylogenetic analysis of mitochondrial DNA sequences. *Molecular Phylogenetics and Evolution* 1995;**4**:93–102.

Fouquet A, Leblanc K, Framit M *et al*. Species diversity and biogeography of an ancient frog clade from the Guiana Shield (Anura: Microhylidae: *Adelastes*, *Otophryne*, *Synapturanus*) exhibiting spectacular phenotypic diversification. *Biological Journal of the Linnean Society* 2021;**132**:233–56.

Gomes DF, Azevedo J, Murta-Fonseca R *et al*. Taxonomic revision of the genus *Xenopholis* Peters, 1869 (Serpentes: Dipsadidae): integrating morphology with ecological niche. *PLoS One* 2020;**15**:e0243210.

Gibbs AK, Barron CN. *The geology of the Guiana Shield*. Oxford: Oxford University Press, 1993.

Grazziotin FG, Zaher H, Murphy RW *et al*. Molecular phylogeny of the New World Dipsadidae (Serpentes: Colubroidea): a reappraisal. *Cladistics* 2012;**28**:437–59.

Hedges SB. Molecular evidence for the origin of birds. *Proceedings of the National Academy of Sciences of the United States of America* 1994;**91**:2621–4.

Heinicke MP, Duellman WE, Trueb L *et al*. A new frog family (Anura: Terrarana) from South America and an expanded direct-developing clade revealed by molecular phylogeny. *Zootaxa* 2009;**2211**:1–35.

Hoang DT, Chernomor O, von Haeseler A *et al*. UFBoot2: improving the ultrafast bootstrap approximation. *Molecular Biology and Evolution* 2018;**35**:518–22.

Hofstadler-Deiques C, Lema T. On the cranial morphology of *Elapomorphus*, *Phalotris* and *Apostolepis* (Serpentes: Colubridae), and its phylogenetic significance. *Zootaxa* 2005;**1042**:1–26.

Hoge AR, Federsoni PA. Notes on *Xenopholis* Peters and *Paraoxyrophus* Schenkel (Serpentes: Colubridae). *Memórias do Instituto Butantan* 1974;**38**:137–46.

Hoogmoed MS. Revision of the genus *Atractus* in Surinam, with the resurrection of two species (Colubridae, Reptilia). *Zoologische Verhandelingen* 1980;**175**:1–47.

Hoogmoed MS, Fernandes R, Kucharzewski C *et al*. Synonymization of *Uromacer ricardinii* Peracca, 1897 with *Dendrophis aurata* Schlegel, 1837 (Reptilia: Squamata: Colubridae: Dipsadinae), a rare South American snake with a disjunct distribution. *South American Journal of Herpetology* 2019;**14**:88–102.

Huber O. Geographical and physical features. In: Berry PE, Holst BK, Yatskievych K (eds.), *Flora of the Venezuelan Guayana*, Vol. **1**. St. Louis: Missouri Botanical Garden Press, 1995, 1–61.

Jansen M, Álvarez LG, Koehler G. Description of a new species of *Xenopholis* (Serpentes: Colubridae) from the Cerrado of Bolivia, with comments on *Xenopholis* scalaris in Bolivia. *Zootaxa* 2009;**2222**:31–45.

Kalyaanamoorthy S, Minh BQ, Wong TKF *et al*. ModelFinder: fast model selection for accurate phylogenetic estimates. *Nature Methods* 2017;**14**:587–9.

Katoh K, Standley DM. MAFFT multiple sequence alignment software version 7: improvements in performance and usability. *Molecular Biology and Evolution* 2013;**30**:772–80.

Knight A, Mindell DP. On the phylogenetic relationship of Colubrinae, Elapidae, and Viperidae and the evolution of front-fanged venom systems in snakes. *Copeia* 1994;**1994**:1–9.

Koch C, Venegas PJ. A large and unusually colored new snake species of the genus *Tantilla* (Squamata; Colubridae) from the Peruvian Andes. *PeerJ* 2016;**4**:e2767.

Kocher TD, Thomas WK, Meyer A *et al*. Dynamics of mitochondrial DNA evolution in animals: amplification and sequencing with conserved primers. *Proceedings of the National Academy of Sciences of the United States of America* 1989;**86**:6196–200.

Kok PJR. A new genus and species of gymnophthalmid lizard (Squamata: Gymnophthalmidae) from Kaieteur National Park, Guyana. *Bulletin de L'Institut Royal des Sciences Naturelles de Belgique, Biologie* 2005;**75**:35–45.

Kok PJR. A new snake of the genus *Atractus* Wagler, 1828 (Reptilia: Squamata: Colubridae) from Kaieteur National Park, Guyana, northeastern South America. *Zootaxa* 2006;**1378**:19–35.

Kok PJR. A new species of *Oreophrynella* (Anura: Bufonidae) from the Pantepui region of Guyana, with notes on *O. macconnelli* Boulenger, 1900. *Zootaxa* 2009a;**2071**:35–49.

Kok PJR. Lizard in the clouds: a new highland genus and species of Gymnophthalmidae (Reptilia: Squamata) from Maringma tepui, western Guyana. *Zootaxa* 2009b;**1992**:53–67.

Kok PJR. A new species of *Chironius* Fitzinger, 1826 (Squamata: Colubridae) from the Pantepui region, northeastern South America. *Zootaxa* 2010;**2611**:31–44.

Kok PJR. *Islands in the sky: species diversity, evolutionary history, and patterns of endemism of the Pantepui herpetofauna*. *D.Phil. Thesis*, Leiden University, 2013.

Kok PJR. A new species of the Pantepui endemic genus *Riolama* (Squamata: Gymnophthalmidae) from the summit of Murisipántepui, with the erection of a new gymnophthalmid subfamily. *Zoological Journal of the Linnean Society* 2015;**174**:500–18.

Kok PJR, Russo VG, Ratz S *et al*. On the distribution and conservation of two 'Lost World' tepui summit endemic frogs, *Stefania ginesi* Rivero, 1968 and *S. satelles* Señaris, Ayarzagüena, and Gorzula, 1997. *Amphibian & Reptile Conservation* 2016;**10**:5–12.

Kok PJR, Russo VG, Ratz S *et al.* Evolution in the South American 'Lost World': insights from multilocus phylogeography of stefanias (Anura, Hemiphractidae, *Stefania*). *Journal of Biogeography* 2017;**44**:170–81.

Lanfear R, Frandsen PB, Wright AM *et al.* PartitionFinder 2: new methods for selecting partitioned models of evolution for molecular and morphological phylogenetic analyses. *Molecular Biology and Evolution* 2017;**34**:772–3.

Lawson R, Slowinski JB, Crother BI *et al.* Phylogeny of the Colubroidea (Serpentes): new evidence from mitochondrial and nuclear genes. *Molecular Phylogenetics and Evolution* 2005;**37**:581–601.

Leaché AD, McGuire JA. Phylogenetic relationships of horned lizards (*Phrynosoma*) based on nuclear and mitochondrial data: evidence for a misleading mitochondrial gene tree. *Molecular Phylogenetics and Evolution* 2006;**39**:628–44.

Lema T, Hofstadler-Deiques C. Description of a new genus for allocation of *Elapomorphus lepidus* and the status of *Elapomorphus wuchereri* (Serpentes: Dipsadidae: Xenodontinae: Elapomorphini). *Neotropical Biology and Conservation* 2010;**5**:113–9.

Lynch JD. Leptodactylid frogs of the genus *Eleutherodactylus* from the Andes of southern Ecuador. *University of Kansas Museum of Natural History Miscellaneous Publication* 1979;**66**:1–62.

Maddison WP, Maddison DR. Mesquite: a modular system for evolutionary analysis. [Computer software]. Version 3.10. http://mesquiteproject.org. 2016.

Mayr E, Phelps WH. The origin of the bird fauna of the south Venezuelan highlands. *Bulletin of the American Museum of Natural History* 1967;**136**:269–328.

McDiarmid RW, Donnelly MA. The herpetofauna of the Guayana highlands: amphibians and reptiles of the Lost World. In: Donnelly MA, Crother BI, Guyer C, *et al.* (eds.), *Ecology and Evolution in the Tropics: a Herpetological Perspective*. Chicago: University of Chicago Press, 2005, 461–560.

Miller MA, Pfeiffer W, Schwartz T. Creating the CIPRES Science Gateway for inference of large phylogenetic trees. In: Proceedings of the Gateway Computing Environments Workshop (GCE), 14 November 2010. New Orleans, LA: Institute of Electrical and Electronics Engineers (IEEE), 2010, 1–8.

Mira-Mendes CV, Oliveira RM, Ruas DS *et al.* *Xenopholis scalaris* (Wucherer's Ground Snake). Defensive behavior. *Herpetological Review* 2013;**44**:699.

Moraes LJCL, Entiauspe-Neto OM, de Fraga R *et al.* Systematics of the rare Amazonian genus *Eutrachelophis* (Serpentes: Dipsadidae), with an emended diagnosis for *Eutrachelophis papilio*. *Zoologischer Anzeiger* 2021;**295**:191–204.

Myers CW. A new genus for Andean snakes related to *Lygophis boursieri* and a new species (Colubridae). *American Museum Novitates* 1973;**2522**:1–37.

Myers CW. New generic names from some neotropical poison frogs (Dendrobatidae). *Papéis Avulsos de Zoologia, São Paulo* 1987;**36**:301–6.

Myers CW. A new genus and new tribe for *Enicognathus melanauchen* Jan, 1863, a neglected South American snake (Colubridae: Xenodontinae), with taxonomic notes on some Dipsadinae. *American Museum Novitates* 2011;**3715**:1–33.

Myers CW, Donnelly MA. Herpetofauna of the Yutajé-Corocoro massif, Venezuela: second report from the Robert G. Goelet American Museum's Terramar expedition to the northwestern tepuis. *Bulletin of the American Museum of Natural History* 2001;**261**:1–85.

Myers CW, McDowell SB. New taxa and cryptic species of Neotropical snakes (Xenodontinae), with commentary on hemipenes as generic and specific characters. *Bulletin of the American Museum of Natural History* 2014;**385**:1–112.

Olson DM, Dinerstein E, Wikramanayake ED *et al.* Terrestrial ecoregions of the world: a new map of life on Earth. *BioScience* 2001;**51**:933–8.

Palci A, Lee MS, Hutchinson MN. Patterns of postnatal ontogeny of the skull and lower jaw of snakes as revealed by micro-CT scan data and three-dimensional geometric morphometrics. *Journal of Anatomy* 2016;**229**:723–54.

Palumbi SR, Martin AP, McMillan WO *et al.* *The Simple Fool's Guide to PCR*. Honolulu: University of Hawaii Press, 1991.

Pellegrino KCM, Brunes TO, Souza SM *et al.* On the distinctiveness of *Amapasaurus*, its relationship with *Loxopholis* Cope 1869, and description of a new genus for *L. guianensis* and *L. hoogmoedi* (Gymnophthalmoidea/Ecpleopodini: Squamata). *Zootaxa* 2018;**4441**:332–46.

Peters JA. The snakes of the subfamily Dipsadinae. *University of Michigan Museum of Zoology Miscellaneous Publications* 1960;**114**:1–228.

Peters JA. *Dictionary of Herpetology*. New York: Hafner, 1964.

Pinheiro PDP, Kok PJR, Noonan BP *et al.* A new genus of Cophomantini, with comments on the taxonomic status of *Boana liliae* (Anura: Hylidae). *Zoological Journal of the Linnean Society* 2018;**185**:226–45.

Pook CE, Wooster W, Thorpe RS. Historical biogeography of the Western Rattlesnake (Serpentes: Viperidae: *Crotalus viridis*), inferred from mitochondrial DNA sequence information. *Molecular Phylogenetics and Evolution* 2000;**15**:269–82.

Priem HN, Boelrijk NA, Hebeda EH *et al.* Age of the Precambrian Roraima Formation in northeastern South America: evidence from isotopic dating of Roraima pyroclastic volcanic rocks in Suriname. *Geological Society of America Bulletin* 1973;**84**:1677–84.

Pyron RA, Burbrink FT, Colli GR *et al.* The phylogeny of advanced snakes (Colubroidea), with discovery of a new subfamily and comparison of support methods for likelihood trees. *Molecular Phylogenetics and Evolution* 2011;**58**:329–42.

Pyron RA, Guayasamin JM, Peñafiel N *et al.* Systematics of Nothopsini (Serpentes, Dipsadidae), with a new species of *Synophis* from the Pacific Andean slopes of southwestern Ecuador. *ZooKeys* 2015;**541**:109–47.

Rambaut A. Figtree, a graphical viewer of phylogenetic trees, 2016. [Computer software]. http://tree.bio.ed.ac.uk/software/gtree.

Rambaut A, Drummond AJ, Xie D *et al.* Posterior summarization in Bayesian phylogenetics using Tracer 1.7. *Systematic Biology* 2018;**67**:901–4.

Raven PH, Gereau RE, Phillipson PB *et al.* The distribution of biodiversity richness in the tropics. *Science Advances* 2020;**6**:eabc6228.

Rivero JA. Notes on the genus *Cryptobatrachus* (Amphibia, Salientia) with the description of a new race and four new species of a new genus of hylid frogs. *Caribbean Journal of Science* 1968;**6**:137–49.

Ronquist F, Teslenko M, van der Mark P *et al.* MrBayes 3.2: efficient Bayesian phylogenetic inference and model choice across a large model space. *Systematic Biology* 2012;**61**:539–42.

Señaris JC, Ayarzagüena J, Gorzula SJ. Los sapos de la familia Bufonidae (Amphibia: Anura) de las tierras altas de la Guayan Venezolana: descripción de un nuevo género y tres especies. *Publicaciones de la Asociación de Amigos de Doñana, Sevilla* 1994;**3**:1–37.

Santos JOS, Potter PE, Reis NJ, Hartmann LA, Fletcher IR, McNaughton NJ. Age, source, and regional stratigraphy of the Roraima Supergroup and Roraima-like outliers in northern South America, based on U-Pb geochronology. *Geological Society of America Bulletin* 2003;**115**(3):331–348.

Steyermark JA. Flora of the Guayana Highland: endemicity of the generic flora of the summits of the Venezuelan tepuis. *Taxon* 1979;**28**:45–54.

Steyermark JA. Relationship of some Venezuelan forest refuges with lowland tropical floras. In: Prance GT (ed.), *Biological Diversification in the Tropics, Proceedings of the Fifth International Symposium of the Association for Tropical Biology*. New York: Columbia University Press, 1982, 182–220.

Synnott M. Up the mountain to a world apart. *National Geographic Magazine*, 2022, 36–71.

Trifinopoulos J, Nguyen LT, von Haeseler A *et al.* W-IQ-TREE: a fast online phylogenetic tool for maximum likelihood analysis. *Nucleic Acids Research* 2016;**44**:W232–5.

Uetz P. The Reptile Database, 2022. http://www.reptile-database.org (20 December 2022, date last accessed).

Uzzell TA. Revision of the genus *Prionodactylus* with a new genus for *P. leucostictus* and notes on the genus *Euspondylus* (Sauria, Teiidae). *Postilla* 1973;**159**:1–67.

Vacher J-P, Kok PJR, Rodrigues MT *et al.* Cryptic diversity in Amazonian frogs: integrative taxonomy of the genus *Anomaloglossus* (Amphibia:

Anura: Aromobatidae) reveals a unique case of diversification within the Guiana Shield. *Molecular Phylogenetics and Evolution* 2017;**112**:158–73.
Vidal N, Dewynter M, Gower DJ. Dissecting the major American snake radiation: a molecular phylogeny of the Dipsadidae Bonaparte (Serpentes, Caenophidia). *Comptes Rendus Biologies* 2010;**333**:48–55.
Wallach V, Williams KL, Boundy J. *Snakes of the World: a Catalogue of Living and Extinct Species*. London and New York: CRC Press, 2014.
Zaher H. Hemipenial morphology of the South American xenodontine snakes, with a proposal for a monophyletic Xenodontinae and a reappraisal of colubroid hemipenes. *Bulletin of the American Museum of Natural History* 1999;**240**:1–168.
Zaher H, Murphy RW, Arredondo JC *et al*. Large-scale molecular phylogeny, morphology, divergence-time estimation, and the fossil record of advanced caenophidian snakes (Squamata: Serpentes). *PLoS One* 2019;**14**:1–82.
Zaher H, Grazziotin FG, Cadle JE, Murphy RW, de Moura JC, Bonatto SL. Molecular phylogeny of advanced snakes (Serpentes, Caenophidia) with an emphasis on South American xenodontines: a revised classification and descriptions of new taxa. *Papéis Avulsos de Zoologia* 2009;**49**:115–153.
Zaher H, Prudente AL. The enigmatic Amazonian genus *Eutrachelophis*: morphological evidence and description of new taxa (Serpentes: Dipsadidae: Xenodontini). *Amphibia-Reptilia* 2020;**41**:215–31.